

WIND FORCES ON OPEN OR
UMBRELLA-TYPE SHELTERS

By

Charles Edward Rice

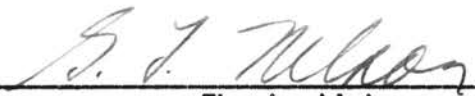
Bachelor of Science in Agricultural Engineering
Oklahoma State University
Stillwater, Oklahoma
1960

Submitted to the faculty of the Graduate School
of the Oklahoma State University of
Agriculture and Applied Science
in partial fulfillment of the
requirements for the degree
of
MASTER OF SCIENCE
May, 1961


OCT 11 1961


WIND FORCES ON OPEN OR
UMBRELLA-TYPE SHELTERS

Thesis Approved:



Thesis Adviser





Dean of the Graduate School

472851

ACKNOWLEDGEMENT

The writer wishes to express his appreciation to those who aided him in this investigation.

The valuable guidance, assistance, and encouragement of Dr. Gordon L. Nelson throughout the entire program is greatly appreciated.

The writer is indebted to Oklahoma State University and the Oklahoma Experiment Station for their financial support which made the study possible.

Recognition should be given to A. P. Juhlin of the Oklahoma State University Library for his assistance in obtaining certain publications.

The writer appreciates the support and suggestions offered by members of the Agricultural Engineering Department. The writer also wishes to thank the drafting department of the Agricultural Engineering department for their help in preparing the charts and graphs.

The writer also wishes to thank his wife, La Donna, for her support and patience during the past four years.

TABLE OF CONTENTS

Chapter	Page
I. INTRODUCTION	1
II. REVIEW OF LITERATURE	5
Wind Structure	5
Windstorm Types and Characteristics	13
Barrier Effects	17
Similiarity Requirements	20
Testing Methods	23
Wind Force Effects on Buildings	24
III. THE STUDY	26
Objective	26
Assumptions	26
Pertinent Quantities	28
Formation of Pi Terms	30
Experimental Design	32
IV. EXPERIMENTAL EQUIPMENT	37
Wind Tunnel	37
Model Roof Components	37
Barriers	39
Model Mast Supports	39
Force Sensing Devices	41
Model Installation	41
Velocity Measuring Equipment	44
Apparatus For The Two-Dimensional Wind Profile	44
V. PROCEDURE	52
Determination Of The Velocity Distribution In The Wind Tunnel	52
General Procedure For Conducting Experiments	53
VI. ANALYSIS OF DATA	56
Calculation Of Wind Velocities	56
Calculation of Π_B Parameters	57
Calculation of Π_q Parameters	57
Statistical Analyses	59

Chapter	Page
VII. DISCUSSION OF RESULTS	62
Statistical Analyses	63
Effect Of Roof Slope	63
Effect Of Shelter Height	65
Effect Of Shelter Length	66
Effect Of Upwind Barriers	66
Reynolds Number	70
Comparison Of One-Dimensional And Two-Dimen- sional Velocity Profiles	70
Comparison Of \bar{U}_q As Found By; Present Data, ARS Data, and Irminger and Nøkkentved's Data	71
Application Of Experimental Results	74
Oscillatory Forces	75
VIII. SUMMARY AND CONCLUSIONS	79
Suggestions For Futher Investigations	81
SELECTED BIBLIOGRAPHY	82
APPENDIXES	85
Appendix A	86
Appendix B	93

LIST OF TABLES

Table	Page
I. Pertinent Quantities	29
II. Parameter Combinations	33
III. Parameter Combinations for the Statistical Analyses	60
IV. Summary Table of the Variance Ratios and Significance Levels Associated With Differences in π_B , the Parameter Defining the Location of Zero Bending Moment	61
V. Summary Table of the Variance Ratios and Significance Levels Associated With Differences in π_q , the Wind Force Parameter	61
VI. Mean Values for π_B , the Parameter Defining the Location of Zero Bending Moment, and π_q , the Wind Force Parameter	64
VII. Comparison of the π_B and π_q values obtained with a One- Dimensional Wind Profile and a Two-Dimensional Wind Profile	71
VIII. Comparison of π_q Values, The Wind Force Parameter, Obtained With: Present Experimental Data, ARS Data, and Irminger and Nøkkentved's Data	73
IX. Oscillatory Force Data	78

LIST OF FIGURES

Figure	Page
1. Umbrella-Type Hay Storage Shelter	2
2. Umbrella-Type Cattle Shade	2
3. Definition Sketch of System	31
4. Dimensionless Parameters	31
5. The Agricultural Engineering Research Wind Tunnel	38
6. Definition Sketch of Model Roof Component	40
7. Definition Sketch of Barrier	42
8. Definition Sketch of Model Mast Support	43
9. Anchors For Model Mast Supports	45
10. Mast Supports Installed in Wind Tunnel	45
11. Definition Sketch of Shield for Model Mast Support	46
12. Precision Manometer Used for Obtaining the Static Pressures	47
13. Relationship Between the Static Pressure and the Velocity Head at the Test Installation	48
14. Size and Arrangement of Rods Used to Obtain the Two-Dimensional Wind Profile	50
15. Slope of the Two-Dimensional Wind Profile on Log-Log Paper	51
16. Typical Model Installation in the Wind Tunnel	54
17. Bridge Balancing Unit and Strain Indicator	54
18. Typical Moment Diagram for the Model Mast Support	58
19. Typical Plot of the Shear Versus the Velocity Squared	58
20. Π_3 as a Function of Π_4 for a Ventilated Barrier	68

Figure	Page
21. π_8 as a Function of π_4 for a Solid Barrier	68
22. π_9 as a Function of π_4 for a Ventilated Barrier	69
23. π_9 as a Function of π_4 for a Solid Barrier	69
24. Equipment used to Obtain the Oscillograph Traces	76

CHAPTER I

INTRODUCTION

Open or umbrella-type shelters are coming into widespread use for agricultural, industrial, and military purposes throughout the United States, especially in regions with long, hot summers and relatively mild winters. An open or umbrella-type shelter is simply a roof section supported by masts. Two typical umbrella-type shelters are illustrated in figures 1 and 2. Agricultural uses of these shelters include livestock shades, livestock feeding shelters, hay and machinery storage shelters. The shelters are simple, economical, and permit easy access to the shelter space by livestock and equipment.

Since open or umbrella-type shelters are a relatively new type of structure on farms throughout the United States, little or no information is available on the forces on the shelters due to wind. This information must be available to persons responsible for the design and construction of open or umbrella-type shelters if the damage due to windstorms is to be reduced to a minimum. Every year in some parts of the United States windstorms cause a large toll of needless damage to farm structures. Dodge and Molander (6, pp. 1-32) reported on the damage by hurricane Hazel which occurred in October, 1954, in the Northeast section of the United States. Hurricane Hazel caused property and crop damage in excess of \$250 million(6, p. 3). More than 2,000 poultry houses were destroyed on the Eastern shore of Delaware and

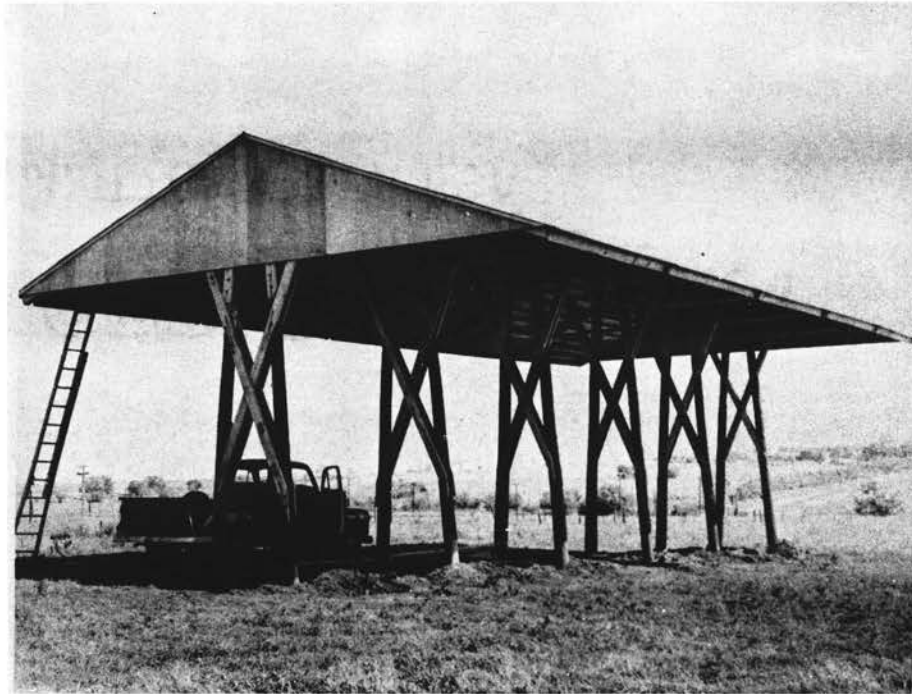


Figure 1 - Umbrella-Type Hay Storage Shelter

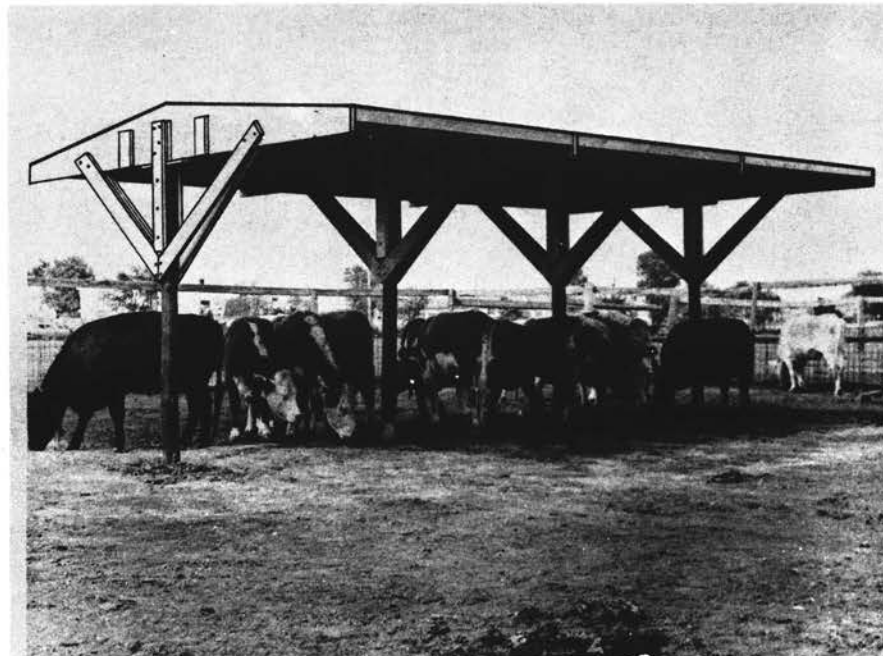


Figure 2 - Umbrella-Type Cattle Shade

Maryland, and more than 700 tobacco barns were destroyed in Maryland. Otis (15, pp. 115-118) reported total damage to real property estimated at \$2 million for a storm that swept through Minnesota on Sept. 11, 1942.

It is possible that much of this damage could have been prevented by such things as more personal attention to the structures, keeping the structures in good repair, removing objects in the vicinity that are too weak to resist strong winds, and most important, incorporating the elements of good construction that make for strength in the original structures at the time they are built.

Persons who design umbrella-type shelters require accurate information on the shears and bending moments in the masts or supports due to wind. Reliable information of this type has not been available. For instance, one method (21, p. 279) commonly used for calculating the horizontal and overturning wind forces specifies a certain minimum wind pressure for the vertical projection of the roof. This method yields an unrealistic estimate of the magnitude and location of the maximum bending moment, and usually results in overdesigned masts at the ground and underdesigned masts and connections at the juncture of the masts and roof. Also, little or no information is available on the effect of configuration factors such as shelter height, shelter length, and upwind barriers on wind forces on open or umbrella-type shelters.

The present study was undertaken to obtain data on the gross horizontal and overturning wind forces on open or umbrella-type shelters exposed to a wind blowing normal to the length of the shelter. An experimental investigation of the gross horizontal and overturning wind forces on umbrella-type shelters was conducted, using models in a wind tunnel,

exposed to a one-dimensional flow pattern blowing normal to the length of the models. The effects of variations in roof slope, shelter length, shelter height, and upwind barriers were investigated. Upwind barriers may include fences, trees, and other structures which may often be present on farms.

The model experiments were organized and conducted according to the principles of similitude. The validity of the results depends upon the correct application of the principles of similitude and the selection of the quantities pertinent to the study.

CHAPTER II

REVIEW OF LITERATURE

Wind Structure

It is a well known and accepted fact that wind speed varies with height above the ground. This variation is not necessarily the same from one geographic location to another, and from one time of occurrence to another. Considerable research has been done on this subject, and many contributions have been made by investigators in the fields of theoretical and applied mechanics, meteorology, micrometeorology, and climatology.

Boundary Layer Theory

Much of the work done on this subject has been based on Prandtl's developments in boundary layer theory. Prandtl (17) prepared a rational development for the variation of velocity with height above a flat plate for fluid flow in which shearing stresses exist in the boundary layer due to momentum transfer as well as viscous forces. His development is based on the momentum theorem for two-dimensional flow with irregular fluctuations which is, however, steady on the average. Prandtl (p. 117) found that stresses arise with variations in velocity due to the momentums arising from these velocity variations. These shear stresses are, $\tau = -\rho u'v'$, where τ is the shear stress, ρ is the fluid density, and u' and v' are the deviations of u and v , the components of velocity

from their average values, u_m and v_m . He found that v' must be of the order $l \frac{\partial u_m}{\partial Y}$ and stated the expression for stress due to momentum transfer as

$$\tau' = \rho l^2 \left| \frac{\partial u_m}{\partial Y} \right| \frac{\partial u_m}{\partial Y}$$

or

$$\tau' = A \frac{\partial u_m}{\partial Y}$$

where, A = exchange coefficient,

τ' = unit shearing stress due to momentum transfer,

ρ = density of the fluid,

l = mixing length,

u_m = mean velocity in horizontal direction,

Y = vertical ordinate.

Prandtl then gives the expression for total shearing stress as

(p. 124)

$$\tau = \mu \frac{\partial u_m}{\partial Y} + \rho l^2 \left(\frac{\partial u_m}{\partial Y} \right)^2$$

where, μ = viscosity of the fluid,

τ = total shearing stress due to the mean value of viscous stress plus the apparent shearing stress due to turbulence.

For fully developed turbulent flow the first term may be neglected, and taking the square root of the resulting equation (p. 124)

$$\sqrt{\tau/\rho} = l \frac{\partial u_m}{\partial Y}$$

where, $v_* = \sqrt{\tau/\rho}$ = shearing stress velocity which may be constant.

Prandtl assumed that l was unaffected by viscosity, and that u_m was steady and two-dimensional. With these assumptions, the equation was put in the solvable form (p. 125)

$$v_* = k Y \frac{du}{dY}$$

where, $K = l/Y$

This equation can be solved giving (p. 125)

$$u = V_* \left(\frac{1}{K} \log Y + C \right)$$

Prandtl obtained an expression for C from the fact that the viscosity becomes important in the immediate neighborhood of the wall. He did this with the use of a length characteristic of flow close to the wall equal to $\sqrt{\nu/V_*}$, where ν is the kinematic viscosity. Prandtl presented the following general expression for variation of velocity with distance from the plane assuming the air has uniform density (p. 126)

$$u = V_* \left(\frac{1}{K} \log \left[Y V_* / \sqrt{\nu} \right] + C_1 \right)$$

where, u = velocity at height Y ,

$V_* = \sqrt{\tau/\rho}$ = shearing stress velocity,

τ = shearing stress,

ρ = density of fluid,

$K = l/Y$

l = mixing length,

C_1 = universal constant.

Prandtl (p. 127) found, as an approximation for the lower region of turbulence, that the velocity will vary as the seventh root of the distance from the boundary, for Reynolds number up to 10^5 . For greater values of Reynolds number, Prandtl found that the velocity is proportional to the eighth, ninth, and tenth roots of the distance from the boundary.

Prandtl concluded that as the wind velocity increases, the height of the frictional layer increases in proportion to it. For turbulent flow for wind speed as a function of the height above the ground, he gave the expression (p. 359)

$$U = V_* \left(5.75 \log_{10} \frac{Z}{K} + C_2 \right)$$

where, U = wind velocity at height Z ,

Z = height above the ground,

C_2 = universal constant which varies between 5.0 and 8.5,

K = height of irregularities such as houses and vegetation,

V_* = shearing stress velocity.

Experimental Investigations

Geiger (7, pp. 103-106) favored the power law for expressing the variation of wind velocity with height above the ground. The power law expression is (p. 103)

$$V_2 = V_1 Z^\alpha$$

where, V_2 = velocity at height Z ,

V_1 = velocity at some reference height,

α = exponent, whose value is obtained from observations.

Geiger concluded that α is not constant, but its value depended primarily on height. When height increased, the effect of ground friction diminished, and α became smaller (p. 105). He referred to Hellman's observations that in reference to the air near the ground that, for at least the lowest 1-1/2 meters, α may be considered as constant (p. 105). He presented evidence that α must be dependent on the temperature, for during the summer months α varied from 0.07 at midday to 0.17 at midnight, and during the winter months α varied from 0.08 at midday to 0.13 at midnight. From this he concluded that it is impossible to separate the effects of temperature gradient and wind gradient for they mutually affect and determine one

another.

For the power law Sutton (22, pp. 230-233) suggested values for the exponent for diurnal variations, varying from about 1/6 in large inversions to about 1/14 in large lapse rates. He referred to the work of Scrase who found during periods of very small temperature gradients, the wind profile between the heights of three and 13 meters was adequately represented by the power law with the exponent equal to 0.13. This is virtually the same profile as the well known seventh-root law of variation of wind speed with height in a turbulent boundary layer for a flat plate as suggested by Prandtl.

Sutton (22, pp. 230-233) suggested that for analysis of the wind structure in the lower layer of the atmosphere, it is advantageous to regard the air at these levels as part of a fully developed turbulent boundary layer. For air of uniform density and smooth flow, Sutton presented Prandtl's expression

$$\frac{u}{V_*} = \left(\frac{1}{K} \log \frac{V_* z}{\nu} + C \right)$$

For fully rough flow he gave the expression

$$\frac{u}{V_*} = \frac{1}{K} \ln \frac{z}{z_0}$$

where, $V_* = \sqrt{\tau_0/\rho}$ = friction velocity,

z_0 = roughness length,

K = Karman's constant,

ν = kinematic viscosity,

u = velocity at height z .

Sutton included a table giving values for V_* and z_0 for various types of surface conditions (p. 233).

Sherlock (19, pp. 1-26) studied the wind velocity variations with height during a storm with anemometers spaced 25 feet apart on a 250

foot tower. From his results he suggested a value of $1/7$ for the value of the exponent in the power law as being sufficiently close for describing the variation of wind velocity with height up to 1,000 feet.

Singer and Maynard (16, pp. 3-5) criticized Sherlock's data on the variation of wind velocity with height due to the fact that he obtained his observations from only one location. Therefore, they doubted that his data were representative. From wind data obtained at heights of 37, 75, 150, and 410 feet above the ground for a study of 13 storms, Singer and Maynard (p. 5) showed that a value for the exponent of 0.250 gave profiles that were typical of the profiles during strong winds in their location. From studies made by Thomas and Fresen (16, pp. 6-7) at heights of seven, 50, 100, 200, 300, and 400 feet above the ground they recommended 0.185 as the value for the exponent in the power law. Pagon (15, p. 1) suggested a value of 0.167 for the exponent in the power law.

Malina (12, pp. 262-284) proposed that for turbulent unladen air flow over an unobstructed flat surface, the variation of the mean velocity of motion parallel to the surface with height z , is well represented by Prandtl's extension to the atmospheric equation of Von Karman's logarithmic relation

$$u = 5.75 \sqrt{\tau/e} \log_{10} \frac{z}{K}$$

where, u = mean velocity,

τ = friction per unit area acting on the surface,

e = air density,

z = height above the ground,

K = roughness factor, usually taken as $1/30$ or $1/33$ of the average diameter of the surface elements.

Thorntwaite and Halstead (25, pp. 249-255) analysed wind data

observed by the Soil Conservation Service at different levels above the ground surface. They found that there was a systematic departure from the logarithmic law and that a line fitting the points was not straight, but one with slight concave curvature. They concluded that this was due to the fact that the effective height of the anemometer is different from the measured height, and that an effective surface for turbulent transfer exists at a height h_0 above the actual physical ground or water surface (pp. 251-252). From their studies Thornthwaite and Halstead (p. 254) suggested that a law which describes the variation of wind velocity with height more closely than any has hitherto been formulated is a combination of the logarithmic and power laws.

$$u = \left[(\log z - \log z_0) / \log a \right]^{1/p}$$

P is believed to vary between 2.0 with fully developed turbulence, to some value less than 1.0 when turbulence reaches its smallest value.

Due to the fact that eddies and large scale thermal convections distort the velocity profile from the ground upward, Brooks (2, p. 93) concluded that such velocity profile expressions as the power law and logarithmic law are only time averages of erratic instantaneous distributions too complicated to use in their actual state. He found that the logarithmic law derived from concepts of similiarity in isotropic turbulence best describes the wind profile in cases of neutral stability, and that the power law best fits profiles developed under stable conditions.

Brooks (2, p. 94) found that the wind profile is related to the foliage layer which absorbs the drag force of the wind and is rather independent of the sheltered, physical ground surface from which the heights of anemometers are specified. Therefore in order to describe the overhead velocities Brooks suggests that it is necessary to use

corrected anemometer heights taken as if measured from an equivalent zero plane. Introduction of this displacement height, d , of the zero plane above the physical ground surface into the power law expression for the velocity profile, the expression becomes (p. 94)

$$\frac{u_z}{u_1} = \left(\frac{z-d}{z_1-d} \right)^P, \quad z \geq d$$

where, u_z = average horizontal air velocity at height z ,

u_1 = observed velocity at height z_1 ,

P = exponent describing the variation with height.

For neutral stability, small scale turbulence, Brooks (p. 94) gives 1/7 as the value for P .

The logarithmic velocity profile expression with the displacement d , becomes (p. 94)

$$e^{bu} = \left(\frac{z-d}{z_0} \right), \quad (z-d) > 0$$

Recapitulation

From the preceding information it can be seen that the variation of wind velocity with height should be considered in a study of wind effects on open-type shelters. From the experimental investigations on this subject it is found that there is much disagreement between the investigators for the proper expression to use in describing the variation of wind velocity with height.

An expression similar to Prandtl's law would appear to be the expression which best describes the variation of wind velocity with height in most cases, for it is a rational development and has considerable experimental data for wind near the ground to support it. The power law is considered by many investigators as sufficiently accurate

for describing the variation of wind velocity with height. An advantage of the power law over the logarithmic form is its simplicity in use.

The selection of a wind velocity profile for the study of wind effects on structures is left to the judgement of the investigator. The investigator must select an expression from the results of other investigators which he believes will best describe the wind velocity profile best suited for his particular study.

Windstorm Types and Characteristics

Wilson (27, pp. 262-271) classifies windstorms into three basic categories: (1) gales, squalls, and thunderstorms, (2) tornadoes, and (3) hurricanes.

The first group occur in all sections of the country, are generally of short duration, and confined to relatively small areas of the country. They are accompanied by a small and slow drop in barometric pressure, gusty winds, usually rain, and sometimes hail.

Tornadoes are characterized by a rotating cone-like vortex with velocities of probably around 200-300 miles per hour, causing almost total destruction in a narrow path ranging from 200-1,500 feet in width. Wilson (p. 262-271) found that tornadoes occur most frequently in the Midwest and Southern states, but that over a 35 year period they have occurred in 47 states.

Wilson (27, pp. 262-271) defined hurricanes as having wind velocities ranging from 75-125 miles per hour, widths ranging from 75-300 miles, and are accompanied by a slow drop in barometric pressure. This type of storm travels in a northerly direction along either the Gulf or Atlantic coasts.

Wind Speeds

A knowledge of wind speeds is essential to the problem of designing structures. The designer must have some knowledge of the wind speeds the structure might encounter in its lifetime. Therefore, a study of wind speeds is a necessary preliminary to a study on open-type shelters.

Wind data are usually available only through the U. S. Weather Bureau. Court (5, pp. 39-56) lists the wind data gathered by the U. S. Weather Bureau as: (1) maximum speed, the greatest of a five minute interval and (2) extreme speed, the speed of the fastest mile from rotating anemometers such as the pressure type, the pitot-static tube, or the bridled cup anemometer. Court analysed two studies for the Washington D. C. area, the only place where cup and pitot-static anemometers operate side by side, and found that during any period with speeds above 30 miles per hour: (1) the strongest gusts are 1.4 times the extreme speed, and (2) the strongest gusts are about 1.5 times the maximum speed. Court suggested that the U. S. Weather Bureau data should not be used without determining peak winds or gusts to be expected when the mean wind of a given time interval is given.

The strongest wind a structure is likely to encounter is most difficult to determine. The strongest wind a structure might encounter will be due to a tornado. According to Wilson (27, pp. 262-271) winds of 200-300 miles per hour are probably in the cone of a tornado, with widths of 200-1,500 feet. Court (5, pp. 39-56) found that on an average 150 or more tornadoes occur in the United States yearly with a width of path of most being 15-150 yards, and occasionally with widths of path of 10-15 miles. Theakston and Walpole (23, p. 2) described tornadoes as having funnel widths generally from 100-400 yards, and with estimated wind speeds of 300-400 miles per hour at the center.

Court (5, pp. 39-56) found that the chances are about 1/5000 that a tornado will strike any one square mile, even in the tornado area. Therefore, he believes the probability so small, and the problem of withstanding a tornado so great, that such wind speeds need not be considered in designing small structures.

Zingg (29, pp. 11-13) advised that if one is to use the weather bureau data on wind speeds, these data must first be adjusted to a common base, for through the years the weather bureau anemometers have not always remained at the same location. From weather bureau data obtained at Dodge City, Kansas, he found that velocities varied from four to five miles per hour due to relocation of anemometers.

Zingg (p. 13) analysed data from 12 windstorms occurring in 1935 in Western Kansas. He found that the peak of intensity of wind movement came, on the average, at the midpoint of the storm duration. He later confirmed this from a study of additional storms. Zingg (p. 13) found the average duration for the 12 storms studied to be 53 hours, varying from 33 to 72 hours. The average storm had a maximum velocity for one hours' time of 29 miles per hour, with a variation ranging from 23 to 35 miles per hour.

Gusts

Gusts are almost always associated with high wind speeds. Gusts are localized high wind velocities lasting for a short interval of time. Sherlock (19, pp. 1-20) relates gusts to wind speed with the use of a gust factor which he describes as being the ratio of the fastest gust velocity to the five minute average velocity. He gave the following equation for relating the gust factor with height.

$$F_z = F_{30} \left(\frac{30}{z} \right)^{0.0625}$$

where, F_z = gust factor at height z ,

F_{30} = gust factor at height of 30 feet.

Sherlock (p. 14) suggested that the design wind speed chosen will be equal to a five minute velocity multiplied by the gust factor.

From a study of wind speeds Collins (4, pp. 825.1-825.13) gave the following characteristics for the gust factor: (1) the gust factor decreased with increased wind velocities, and (2) there was no dependent relationship evident between elevation and the gust factor, other than that wind speed increases with elevation.

Frequency of Maximum Wind Speeds

The maximum wind speed a structure might encounter in its life is difficult to determine. Some investigators believe the solution to determining this maximum speed can be best determined through a statistical analysis of wind data.

Thom (24, pp. 539.1-539.11) found that engineers have long used extreme wind speeds in various forms to determine design wind pressures and wind loads, and that these wind speeds are often defined simply as the highest speed ever recorded at a particular location. He concluded that this method was unsatisfactory, for the value of this extreme depended on the length of record which varies from station to station, making the design winds a function of other factors than climatic experience. Thom found that with equal length of records the sampling variability for the single extreme is so large that it furnishes only a vague indication of what the design wind should be, and that a more serious weakness of the single extreme may be its indefiniteness in respect

to the risks of winds exceeding it. Thus, Thom (p. 539.2) believes the solution for the selection of design wind speeds must come from a statistical analysis of climatological series of wind data. He prefers to use the extreme values, for these values more nearly represent the speed of relatively short bursts of winds which are assumed to be the most dangerous on structures. Thom suggested that the wind data from weather bureau records be transferred to a standard elevation since some of the instruments at the recording stations have been moved occasionally, resulting in changes in elevation.

Court (5, pp. 45-47) used a method similiar to the one advocated by Thom to analyse wind records over a 37 year period from 25 first-order weather bureau stations. He arrived at a set of design wind speeds for structures of various life expectancies with a 10 per cent calculated risk. This method with a calculated risk appears to be well suited for the design of farm structures, for farm structures are built for relatively short lives.

Barrier Effects

Many farm structures are sheltered by objects such as other structures, trees or fences. These objects can be expected to exert much influence on the winds speeds and wind pressures to which farm structures will be subjected. Therefore, in order to determine the actual wind effects an open-type shelter will be subjected to, the effect of these objects must be considered.

Irminger and Nøkkentved (10, pp. 59-63) have presented results of studies of wind movement as affected by screen or barriers. These studies were conducted with models in a wind tunnel with solid and per-

forated screens of heights equal to the building height and $1/3$ the height of the building. The perforated screens had uniformly distributed holes corresponding to 46 per cent of the total area of the screen. The screens were as wide as the wind tunnel, making the stream flow two-dimensional. The screens were located at distances of 100 mm, 300 mm, 400 mm, and 555 mm from the buildings. The solid screen of height equal to the height of the building caused a pressure coefficient of 69 per cent suction, while without screens a positive pressure of 50 to 60 per cent was found. For a 45 degree roof slope building with a solid or perforated screen with height $1/3$ of building height, the pressure on the roof surfaces increased as much as 2.5 times the value as with no screen. Irminger and Nøkkentved (p. 63) found that the sheltering effect just behind a solid screen is much greater than for a perforated screen, but the lee behind a solid screen soon disappears and is followed by a very disturbed vortex region. Other (p. 63) data indicated the sheltering effect behind the perforated screen was less, but that it was constant for a distance at least eight times the height of the screen.

Jensen (11, ch. 14) has made a study of velocity variations to the lee of artificial screens. He conducted his studies in a wind tunnel using several types of artificial screens including: solid screens, screens with horizontal and vertical rails, screens with horizontal and vertical rails in combination, perforated screens with circular openings, and screens of horizontal circular rods. Jensen (p. 169) found that the shape of the open area had no influence on the sheltering effect provided the open areas were uniformly distributed. Thus, he concluded that the shelter effect is dependent on the percentage of

hole area.

In an area extending from eight to 10 times the height downwind of a solid screen Jensen (p. 172) found a marked eddying with wind velocities of up to 30 per cent of the unobstructed velocity. For screens with 38 per cent hole area there was 90 per cent sheltering effect behind the screen at three times the height of the screen with a 10 per cent effect as far as 39 times the height of the screen (p. 172). For a screen of 50 per cent hole area there was 70 per cent sheltering effect at three times the height of the screen with a 10 per cent effect at 37 times the height of the screen. Jensen concluded that maximum sheltering effect is attained with screens of hole area percentage between 35 and 40 per cent. For screens in combination Jensen (p. 191) found that in most cases there was little difference in sheltering effect between two or three screens and a single screen, and outside an area of six times the height of the screen, no difference was found to exist.

Geiger (7, p. 336) studied the vertical distribution of wind speeds in a 15 meter pine stand. He found the reduction in wind speed is principally in the crown space, and that from the lower limit of the crown down to just above the ground plane there prevailed an astonishingly uniform, gentle air movement. Only below one meter was there another reduction, the speed going to zero at the ground surface.

Investigators (8, pp. 6-7) at the agriculture experiment station at Manhattan, Kansas, found while taking velocity data in the turbulent zone immediately to the leeward of a windbreak of 10 rows of trees and shrubs that part of the 30 second velocities obtained during a 10 minute test period were negative. This indicated that the vel-

ocity streamlines were modified by the barrier, and that the wind was actually moving parallel to, or toward the windbreak. The results of this study showed over 50 per cent velocity reduction to the leeward of the windbreak for a distance of from four to eight times the height of the windbreak, and with 10 to 20 per cent reduction in velocity for distances as far as 28 times the height of the windbreak.

From the foregoing data on the effect of barriers for the reduction of velocity in the vicinity of structures, it seems feasible that a reduction in design wind speed is justifiable if these sheltering objects remain in the vicinity for the life of the structures. This reduction in design wind speed for open-type shelters is impossible to determine and specify, for designs of this nature are usually distributed over wide areas with varying conditions. Thus, if any reduction in wind speed is considered, it will be the responsibility of the designer to exercise his judgement in taking this into account.

Similiarity Requirements

Model Similiarity Requirements

Most information obtained by investigators of wind effects on structures has been obtained by experiments conducted with the use of models in wind tunnels. These models were usually constructed to some convenient scale and subjected to a controlled wind in the tunnel. Some investigators expressed the opinion that Reynolds number has no effect on the study, while others believed that Reynolds number must be considered. Van Erp (26, pp. 1-11) cited the work of G. Eiffel in which he showed that the distribution of pressures observed from model tests on sharp-edged bodies can be transferred directly to any larger

scale regardless of the velocity. Eiffel concluded that there was no scale effect, and that Reynolds number was one. A Reynolds number of one corresponds to "creeping" type laminar flow in which Reynolds number would appear to have a very definite effect on the drag. Castleman and Mirsky (17, p. 3) could find no definite agreement among the various writers on scale effect (Reynolds number). They concluded that the absence of scale effect is equivalent to zero viscosity, and criticized Eiffel's statement that the Reynolds number would be one, and suggested that the absence of scale effect results in a Reynolds number of infinity. They found that early investigators tended to discount scale effect in the case of structures with sharp edges as either absent entirely or negligible, but that later investigators seemed to indicate that scale effect may be of some importance in such cases. However, they suggested that the diversity of opinion is still great, and as yet there appeared to be no critical standard to indicate whether scale effect may be neglected or not.

Irminger and Nøkkentved (10, p. 46) found that the magnitude of the Reynolds number affected the pressure distribution on sharp-edged bodies. They attributed this effect of Reynolds number on pressure distribution to the windward ground friction which created an appreciable windward vortex region.

Bridgman (1, p. 85) discussed the use of Reynolds number in model experiments. Reynolds number is equal to $VL\rho/\mu$, where V is the velocity, L is some length factor, ρ is the air density, and μ is the viscosity. For model studies conducted in air, ρ and μ will be the same for model and prototype. This requires that VL be the same for model and prototype. If this was the case, and the model was 1/20

of the linear dimensions of the prototype, this would then require the velocity for the model study to be 20 times the velocity for the prototype. This is impossible to achieve for model studies of this nature. According to Bridgman (p. 85), if the measurements are made on the resistance of the model at various speeds, and the corresponding values of the function calculated (if the measured resistance are divided by $V^2 \rho$), it will be found that at high values of the wind speed the function will approach asymptotically a constant value. Thus, if it is possible to reach these wind speeds where the function approaches this asymptotic value, the results of the model study should be valid for application to other geometrically similar bodies.

Wind Profile Similiarity Requirements

If valid results are to be obtained from a model study of wind effects on structures, the wind profile used in the study should be the same as that likely to be encountered by the prototype under field conditions. Irminger and Nøkkentved (10, pp. 46-47) found that the relative ground roughness governs the pressure distribution. They suggested using the relation \bar{z}/h , where \bar{z} is the thickness of the boundary layer and h the height of the side face of the building, as an indication to the pressure distribution. Irminger and Nøkkentved found from experiments that the pressure varies greatly with the value of \bar{z}/h . For a 20 degree roof slope, low values of \bar{z}/h result in large suction pressures on the windward roof slopes, while at higher values of \bar{z}/h , small positive pressures exist. For a short building, Irminger and Nøkkentved (p. 51) suggested that the pressure distribution will not be dependent upon \bar{z}/h to as great extent as for an extremely long building. This is because air flows not only over, but

around the building, which tends to decrease the influence of the windward vortex layer. Irminger and Nøkkentved suggested that for designs or specifications which take wind pressure into account, it is necessary to consider the value of z/h .

The selection of a wind profile to use in the study of wind effects on open-type shelters is difficult to determine. There is no general agreement among the investigators as to the nature of the variation of wind velocity with height. Also, the roughness of the ground and the presence of barriers have a pronounced effect on the wind structure.

Testing Methods

Most of the work done previously on studying wind effects on structures has been with the use of models subjected to a controlled wind pattern in wind tunnels. The data were usually obtained by measuring the static pressure at small piezometer holes in the surface of the models. These point pressures were then used to plot pressure contours for the surface of the model. This method is slow and tedious, and the pressure contours are cumbersome to use in analysing the total forces on a structure. This method is not suitable for the study of wind effects on open-type shelters, for the apparatus necessary for obtaining the pressures would interfere with the flow pattern through the shelter.

Irminger and Nøkkentved (10, pp. 64-65) used this method for studying the wind effects on open-type shelters by making the roofs of the models of double plates with a small space between them. The pressures communicated to the hollow space through the holes in the roof

were transferred through hollow columns supporting the roof to the manometer.

Wind Force Effects on Buildings

Wilson (27, pp. 262-271) defined two basic wind forces acting on a building as: (1) an exterior force on the roof and leeward walls which is a suction force, and (2) internal pressures within the building. He listed the orientation of the building with respect to the wind and the slope of the roof as major factors affecting the suction forces, with the size, shape, and height of the building as minor factors. With the wind blowing perpendicular to the sidewalls of a building, the suction is greatest with a flat roof. Wilson (p. 263) found that as the slope of the roof increases, the suction decreases on the windward slope until at about a 30 degree slope there is little or no suction. For steeper roof slopes the wind exerts a downward pressure on the windward slope, and a suction force on the leeward slope of all pitched roof buildings.

Wind pressure data on buildings are usually given in terms of pressure coefficients. For suction forces on main building roofs with slopes of 20 degrees or less, Wilson (27, pp. 262-271) suggested a value of 0.77, and for internal pressures, a value of 0.73.

Irminger and Nøkkentved (10, pp. 64-65) studied the wind effects on an open-type shelter with a 30 degree roof slope and one with a curved roof. They found that the characteristic difference between the sharp-edged and curved roofs was the very low pressure and high suction values obtained for the curved roof. The curved roof was subjected to a greater upward force than the sharp-edged roof. They (p. 65)

found that the difference between pressures on the respective halves of the roofs was greatest for the sharp-edged roof. The sharp-edged roof had a pressure coefficient of 1.34 with a 60 degree angle of incidence, as compared to a pressure coefficient of 1.03 for the curved roof with the same angle of incidence. For the sharp-edged roof Irminger and Nøkkentved (p. 65) found that the pressure was always downward on the windward slope, and that suction always existed on the leeward slope regardless of the angle of incidence.

The Agriculture Research Service (28, pp. 1-4) has prepared a map with isograms of maximum velocity pressures in pounds per square foot, at a height of 30 feet above the ground, for the United States. A table (p. 4) of pressure coefficients has also been prepared for walls, roofs, and eaves. These coefficients varied from 0.77 suction for slopes up to 30 degrees, to 0.58 pressure for slopes of 60 degrees and greater.

CHAPTER III

THE STUDY

Objective

The present study was undertaken to evaluate the gross horizontal and overturning wind forces on open or umbrella-type shelters due to wind. The study was conducted with models in a wind tunnel exposed to a one-dimensional flow pattern blowing normal to the length of the models. A two-dimensional flow pattern, described by the power law with an exponent equal to 0.25, was used for some of the tests and the results obtained using the two-dimensional flow pattern were compared with the results obtained using the one-dimensional flow pattern.

The gross horizontal and overturning wind forces in the mast supports were evaluated as influenced by:

1. shelter length,
2. shelter height,
3. roof slope,
4. presence of barrier or screen.

Assumptions

It was assumed that the results obtained from the model study would be applicable to other geometrically similar objects. The validity of this assumption depends upon the correct application of the principles of similitude and the selection of the pertinent quantities.

Correct application of the principles of similitude requires correct application of the Buckingham Pi theorem.

Buckingham Pi Theorem

The Buckingham Pi theorem is the basic tool of dimensional analysis. Buckingham's theorem is stated as follows (3, p. 345):

If an equation is dimensionally homogeneous, it can be reduced to a relationship among a complete set of dimensionless products.

The theorem is discussed in detail by Buckingham (3, pp. 345-376).

Denoting the dimensionless products as π_1, π_2, \dots etc., any equation which completely describes a relation existing among a number of physical quantities of an equal or smaller number of different kinds can be reduced to the form

$$\phi(\pi_1, \pi_2, \dots \text{etc.}) = 0$$

The π'_s are all the independent dimensionless products of the form A_1^x, A_2^y, \dots etc. that can be made by using the symbols of all the quantities A (3, p. 376).

The number of independent and dimensionless products required to express a relationship among the physical quantities is equal to the number of quantities involved minus the rank of the dimensional matrix for the quantities. The only restrictions placed on the dimensionless products or pi terms are that they be dimensionless and independent.

The first and most important step in the application of the Buckingham Pi theorem is the selection of the pertinent quantities. The validity of the results depends upon the correctness with which the pertinent quantities are selected.

Pertinent Quantities

The physical quantities which were believed to be pertinent to a system consisting of an umbrella-type shelter exposed to an one-dimensional flow pattern are tabulated and described in table I. Figure 3 is a definition sketch illustrating the pertinent quantities.

The selection of most of the pertinent quantities is obvious for a system in which there is the movement of a mass of air. The quantities were selected with the assumption that they were important for a study of wind forces on open or umbrella-type shelters.

The variables D and Z were considered important for they determine the height of the structure above the ground plane. The height of shelter above the ground was expected to affect the flow pattern through the shelter.

The roof slope length S was considered in connection with the separation of flow from the roof surface. The flow will separate at the eaves below some critical roof slope. It is possible that, for some roof slope lengths, the flow may return to the roof surface.

L, l , and P were expected to influence the system because they would determine the reduction of forces on the shelter to the leeward of a barrier placed upwind from the shelter.

The shelter length W was expected to influence the flow pattern, for air not only flows over and through the shelter, but around the ends of the shelter also.

The horizontal shear H, and the point of zero moment y, must be known before the design requirements of the mast supports can be specified.

The air viscosity μ was included as a pertinent quantity. The

TABLE I
PERTINENT QUANTITIES

No.	Symbol	Description	Units	Dimensional Symbol
1.	D	Projected Height, Eaves To Ridge	Ft.	L
2.	S	Roof Slope Length	Ft.	L
3.	Z	Height, Ground Plane To Eaves	Ft.	L
4.	L	Horizontal Distance, Barrier To Front Of Shelter	Ft.	L
5.	W	Building Length	Ft.	L
6.	l	Height Of Barrier	Ft.	L
7.	y	Distance, Eaves To Point Of Zero Moment In Mast Support	Ft.	L
8.	P	Ratio, Open Area Of Barrier To Gross Area	-	-
9.	V	Wind Speed	$\frac{\text{Ft}}{\text{Sec}}$	LT^{-1}
10.	e	Mass Density Of Air	$\frac{\text{Lb}_M}{\text{Ft.}^3}$	ML^{-3}
11.	μ	Viscosity Of Air	$\frac{\text{Lb}_F \cdot \text{Sec.}}{\text{Ft.}^2}$	$FL^{-2}T$
12.	K	Newtonian Constant	$\frac{\text{Lb}_F \cdot \text{Sec}^2}{\text{Lb}_M \cdot \text{Ft}}$	$FL^{-1}M^{-1}T^2$
13.	H	Horizontal Shear In One Mast	Lb_F	F

introduction of viscosity results in the formation of a Reynolds number as one of the dimensionless parameters. Some investigators expressed the opinion that one need not consider Reynolds number for a study on sharp-edged objects. Others expressed doubt. If Reynolds number is considered unimportant, this would indicate that the viscous effects are very small in comparison to the inertia effects.

Another quantity which could have been considered in a study of wind forces on open or umbrella-type shelters is the orientation of the shelter with respect to the wind direction. Irminger and Nøkkentved (10, pp. 64-65) found that for an open-type shelter with a 30 degree roof slope the maximum positive pressure on the windward roof occurred with the wind blowing normal to the length of the shelter. As the angle of incidence was decreased, the pressure on the windward slope decreased, and the suction on the leeward roof slope increased to a maximum for a 60 degree angle of incidence, then decreased to zero for an angle of incidence of zero.

Formation of Pi Terms

Thirteen quantities were considered for the study. The rank of the dimensional matrix was four as is shown below. The dimensional matrix for the quantities is:

	<u>D</u>	<u>V</u>	<u>k</u>	<u>H</u>	<u>S</u>	<u>Z</u>	<u>L</u>	<u>W</u>	<u>l</u>	<u>y</u>	<u>P</u>	<u>e</u>	<u>H</u>
F	0	0	1	1	0	0	0	0	0	0	0	0	1
M	0	0	-1	0	0	0	0	0	0	0	0	1	0
L	1	1	-1	0	1	1	1	1	1	1	0	-3	-2
T	0	-1	2	0	0	0	0	0	0	0	0	0	1

For columns D, V, k, and H, the determinant is:

$$\begin{vmatrix} 0 & 0 & 1 & 1 \\ 0 & 0 & -1 & 0 \\ 1 & 1 & -1 & 0 \\ 0 & -1 & 2 & 0 \end{vmatrix} = -1 \neq 0$$

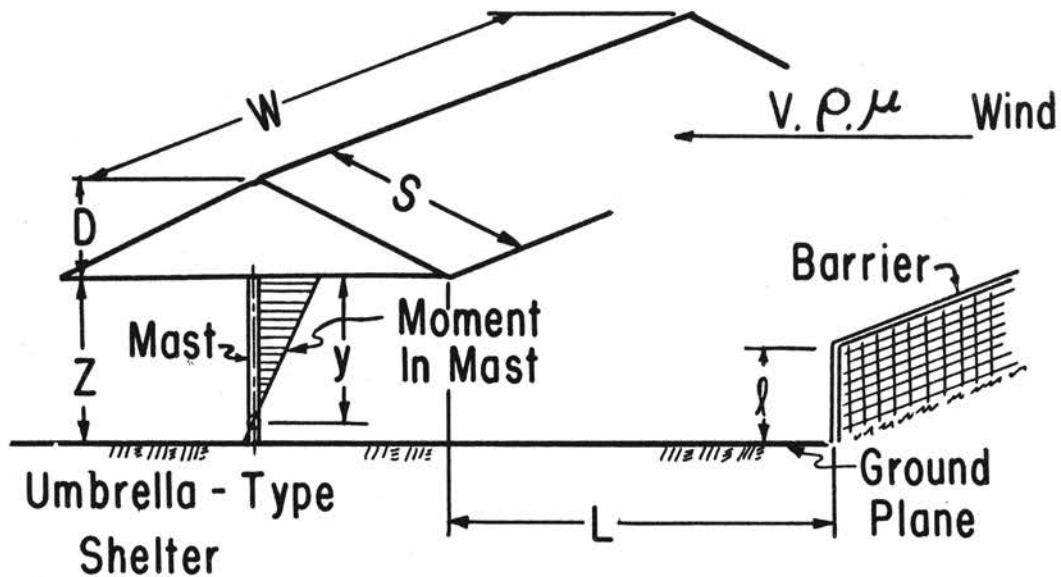


Figure 3. Definition Sketch of System

$$\pi_1 = \frac{D}{S}$$

$$\pi_6 = P$$

$$\pi_2 = \frac{D}{Z}$$

$$\pi_7 = \frac{VD\rho K}{\mu}$$

$$\pi_3 = \frac{D}{W}$$

$$\pi_8 = \frac{Y}{Z}$$

$$\pi_4 = \frac{L}{Z}$$

$$\pi_9 = \frac{2H}{KDWeV^2}$$

$$\pi_5 = \frac{l}{Z}$$

Figure 4. Dimensionless Parameters

Since a fourth order determinant can be formed from the dimensional matrix, this means that the rank of the dimensional matrix is four. With thirteen quantities and the rank of the dimensional matrix equal to four, nine pi terms can be formed from the list of pertinent quantities. The pi terms or dimensionless parameters into which the pertinent quantities were organized are tabulated in figure 4.

Experimental Design

The functional relationships among the pi terms are

$$\begin{aligned}\pi_8 &= f(\pi_1, \pi_2, \dots, \pi_7) \\ \pi_9 &= g(\pi_1, \pi_2, \dots, \pi_7)\end{aligned}$$

where the functions f and g may be determined by analysis of experimental data. Two relationships are necessary among the pi terms since both π_8 and π_9 are dependent pi terms. To evaluate the functions f and g would require holding all the independent pi terms except one constant, and varying that one to establish a relationship between it and the dependent pi terms. This procedure would then have to be repeated for each of the independent pi terms in turn, and the resulting relationships between the dependent pi terms and the other individual pi terms combined to give general relationships. This procedure would require a very elaborate experimental and analytical program. To reduce the study to manageable proportions, experiments were conducted at selected values of the independent pi terms to correspond to typical prototype conditions. The schedules of treatment combinations are tabulated in table II. A brief discussion of the pi terms and the values selected for them follows.

$\pi_1 = D/S$ is essentially a roof slope parameter. π_1 was

TABLE II
PARAMETER COMBINATIONS

No.	π_1	π_3	π_5	π_2	π_4	π_6	
1	0.2425	D = 3 in.	0	1/3			
2				2/3			
3						0	
4			1/10	1/2	1/3	2	.50
5							
6						6	.50
7					2/3	2	0
8							.50
9						6	0
10							.50
11	0.3846	D = 2 in.	0	1/3			
12		1/6	1/2		2	0	
13						.50	
14					6	0	
15						.50	
16			D = 3 in.	0	1/3		
17					2/3		
18				1/2	1/3	1	0
19							
20						2	0
21							.50
22						4	0
23							.50
24					1/3	6	0
25							.50
26			1/10	1/2	2/3	8	0
27							
28						10	0
29							.50
30						12	0
31							.50
32						14	0
33							.50
34						16	0
35							.50
36						2	0
37							.50
38					2/3	6	0
39							.50
40			D = 2 in.	0			
41					2	0	
42		1/12	1/2	1/3		.50	
43					6	0	
44						.50	
45		D = 2 in.	0				
46					2	0	
47		1/18	1/2	1/3		.50	
48					6	0	
49						.50	
50	0.5187	D = 3 in.	0	1/3			
51				2/3			
52				1/2	1/3	2	0
53			1/10				
54							6
55							.50
56					2/3	2	0
57							.50
58						6	0
59						.50	

assigned values of 0.2425, 0.3846, and 0.5187 corresponding to roof slopes of 3/12, 5/12, and 7/12, respectively. For closed structures the roof slope has a pronounced effect on the pressures on the roof due to wind. For instance, experiments on windtight models showed that the net pressure on the roof for structures with a 30 degree or less roof slope was an outward pressure for both the windward and leeward roofs. For a roof slope greater than 30 degrees on windtight structures, the net pressure was an outward on the leeward roof and an inward pressure on the windward roof. Irminger and Nøkkentved (10, pp. 64-65) found from experiments on an open shed with a 30 degree roof slope that the pressure on the windward roof was always inward and the pressure on the leeward roof was always outward.

$\pi_2 = D/Z$ was assigned values of 1/3 and 2/3. With a constant D value, this represents two shelter heights, one being twice the height of the other. For a two-dimensional flow pattern it would appear that the wind forces on the shelter would increase as the height of the shelter increased due to the increase in velocity with height.

$\pi_3 = D/W$ dictates the length of the shelter. π_3 was assigned values of 1/6, 1/10, 1/12, and 1/18 corresponding to four different shelter lengths. The length of the shelter can be expected to influence the flow pattern around the shelter. Relatively more air is expected to flow around a shorter shelter thereby reducing the pressure on the shorter shelter as compared to a longer shelter.

$\pi_4 = L/Z$ was assigned values of two and six for all of the shelter configurations. For one shelter configuration, π_4 was assigned additional values of one, four, eight, 10, 12, 14, and 16. The barrier spacing L was expected to have a pronounced effect on the wind

forces on umbrella shelters, for as the distance from a shelter to an upwind barrier increases, the effect of the barrier in reducing velocity at the shelter becomes less important.

$\pi_5 = l/z$ was held constant at a value of 1/2 for all of the model experiments.

$\pi_6 = P$ describes the type of upwind barrier. π_6 was assigned values of zero and 0.50 corresponding to a solid barrier and a ventilated barrier having a uniformly distributed open area of 50 per cent of the gross area of the barrier.

The π_7 equal to $\frac{KVDE}{\mu}$ is a Reynolds number. For the model results to be applicable for prototype structures, the Reynolds number must be in the range such that a function, $\frac{R}{\sqrt{z}l^2e}$, where R is the measured resistance, is constant for changes in Reynolds number. If this is the case, the force on the structure will be independent of Reynolds number.

$\pi_8 = y/z$ is one of the dependent pi terms. Z is a known value for the experiments, but y must be obtained from analysis of experimental data. y, the location of zero bending moment along the axis of the mast, must be known for a complete description of wind forces on the structure.

$\pi_9 = \frac{2H}{KDW_eV^2}$ is the other dependent pi term. Both π_8 and π_9 must be known to describe the forces on the shelter due to wind.

π_9 is a wind force coefficient which gives a value for the total horizontal force or shear on the shelter. π_9 has to be calculated from the analysis of the experimental data.

In table II the parameter combinations are presented. From the table it is found that there are 59 combinations. This means that

there were 59 individual experiments to conduct. Also, a two-dimensional flow pattern was used with treatment combinations 1, 16, and 50. This made a total of 62 experiments. For treatment combination number 10, for example, the experiment was conducted with $\pi_1 = 0.2425$, $\pi_2 = 2/3$, $\pi_3 = 1/10$, $\pi_4 = 6$, $\pi_5 = 1/2$, and $\pi_6 = 0.50$.

For treatment combinations 16, 20, 21, 26, 27, 30, 31, 34, and 35. the transient strain was obtained. These treatment combinations included a system without an upwind barrier, and systems with solid and ventilated upwind barriers at different barrier spacings. These data were obtained to get a comparison between the amplitude of the oscillatory and static forces on the shelter.

CHAPTER IV

EXPERIMENTAL EQUIPMENT

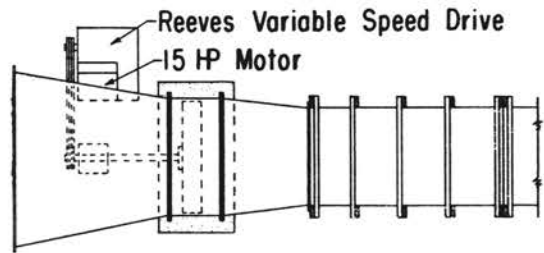
Wind Tunnel

The agricultural engineering wind tunnel located at Oklahoma State University was designed and constructed for low speed testing. The wind tunnel is an open return, induced flow type, with a test section 50 ft long by four ft square, constructed of high density plywood. The tunnel consists of six eight-ft sections and one two-ft section, any one of which may be altered or removed to satisfy the investigator's need. Each eight ft section has a window on either side to permit viewing of any apparatus or equipment installed in the tunnel. The tunnel is driven by a 60 in diameter, 16-bladed, adjustable pitch, axial flow blower. It is powered through a belt drive from a remote controlled, variable speed drive with a 15 hp electric motor. Figure 5 shows the arrangement and major dimensions of the wind tunnel.

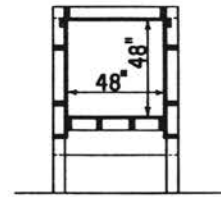
The air circulated through the tunnel can either be recirculated or expelled through an outdoor exhaust. For the present study the laboratory air was continuously recirculated, thus providing fairly constant temperature.

Model Roof Components

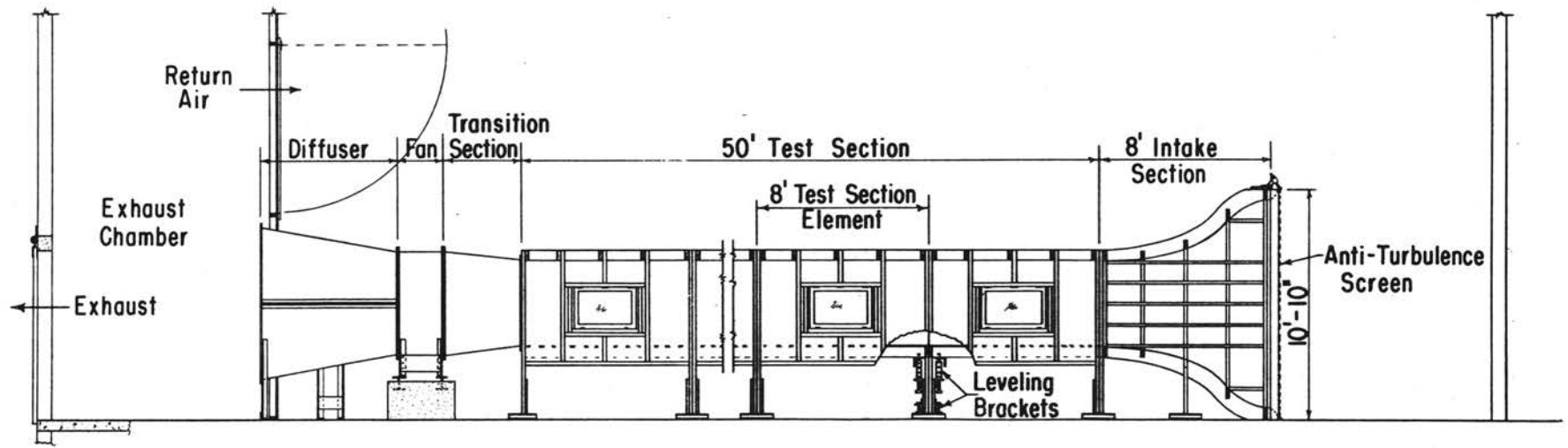
The variations in the model shapes and sizes were obtained by constructing six different roof components. The roof components were



PLAN VIEW - EXHAUST END



CROSS SECTION



ELEVATION - WIND TUNNEL

Figure 5. The Agricultural Engineering Research Wind Tunnel

constructed from 3/16 in mahogany plywood. The sections were assembled by gluing all joints. Small nails were used as the clamping device. The model surfaces were sanded until smooth and two coats of lacquer were applied to all surfaces. Figure 6 is a definition sketch of the model roof components. The dimensions required for the different roof components are tabulated below the diagram.

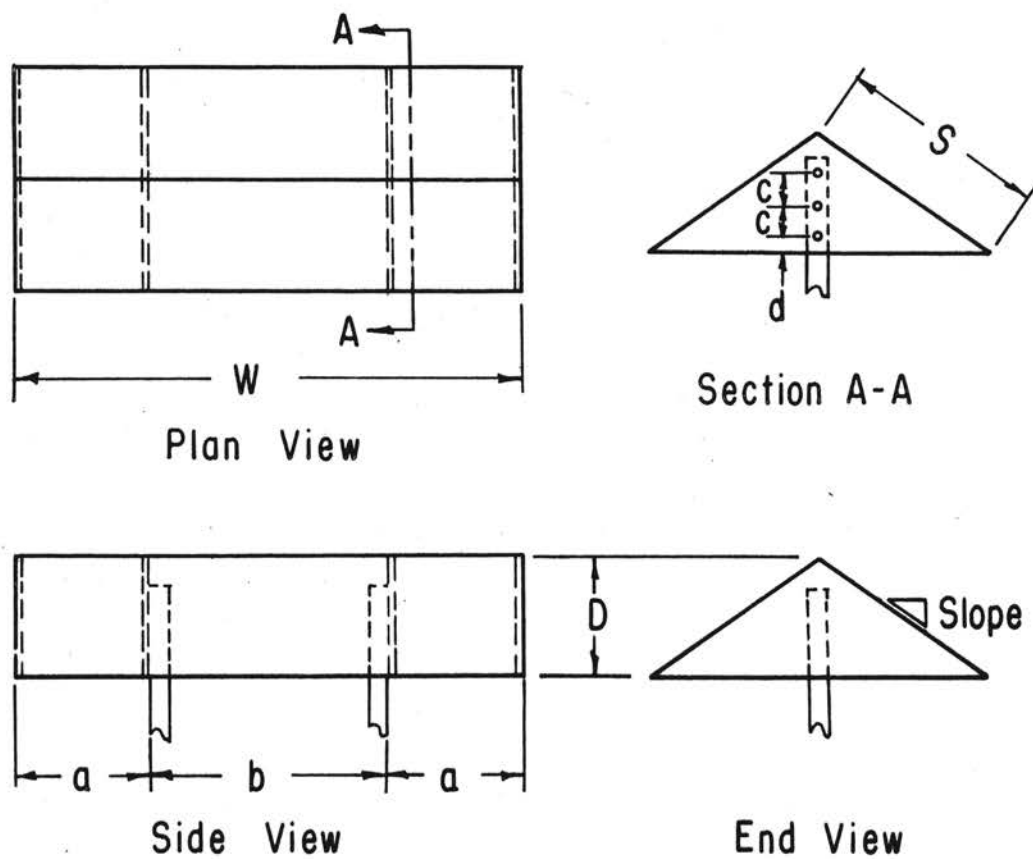
The model roof components were made as large as possible, but had to be kept to a minimum size, for Irminger and Nøkkentved (9,p. 22) found that if the cross sectional area of the model exceeded five to six percent of the cross sectional area of the wind tunnel, the results obtained from the model studies were not dependable. The largest model used in the present study occupied approximately four per cent of the cross section area of the wind tunnel.

Barriers

The solid barriers were constructed of nominal one-inch lumber. They were not sanded or finished. The ventilated barriers were made from stainless steel mesh wire having a uniformly distributed open area of approximately 50 per cent of the gross area of the barrier. The barriers were made as wide as the test section of the wind tunnel, representing an infinite width. The barriers were attached to the tunnel wall at each end with small wood screws. Figure 7 is a definition sketch of a barrier with the dimensions required to satisfy the experimental design tabulated below.

Model Mast Supports

Two pairs of mast supports were required to satisfy the experi-



No.	D in.	Slope	a in.	b in.	S in.	W in.	c in.	d in.
1	3	3/12	7	16	12.37	30	3/4	1/2
2	3	5/12	7	16	7.80	30	3/4	1/2
3	3	7/12	7	16	5.78	30	3/4	1/2
4	2	5/12	0	12	5.18	12	3/4	1/2
5	2	5/12	4	16	5.18	24	3/4	1/2
6	2	5/12	10	16	5.18	36	3/4	1/2

Figure 6. Definition Sketch of Model Roof Component

mental design. The mast supports were constructed from nominal one-inch yellow pine. The size of the model mast supports was decided by the amount of bending needed to obtain sufficient strain in the sensing devices for accurate results. Figure 8 is a definition sketch of a mast support with the dimensions required for each pair tabulated below the diagram.

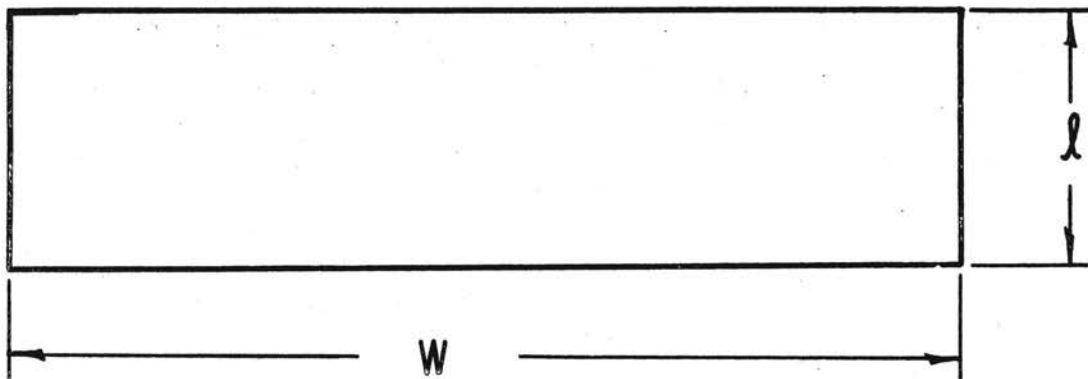
Force Sensing Devices

Electrical resistance strain gages were used as the force sensing devices. Three pair of gages were affixed to each model mast support as shown in figure 8. The gages in each pair were mounted on opposite sides of the mast supports. Before installation in the wind tunnel, the mast supports were loaded as simple cantilever beams to relate strain to bending moment. A calibration curve was drawn for each pair of gages.

Model Installation

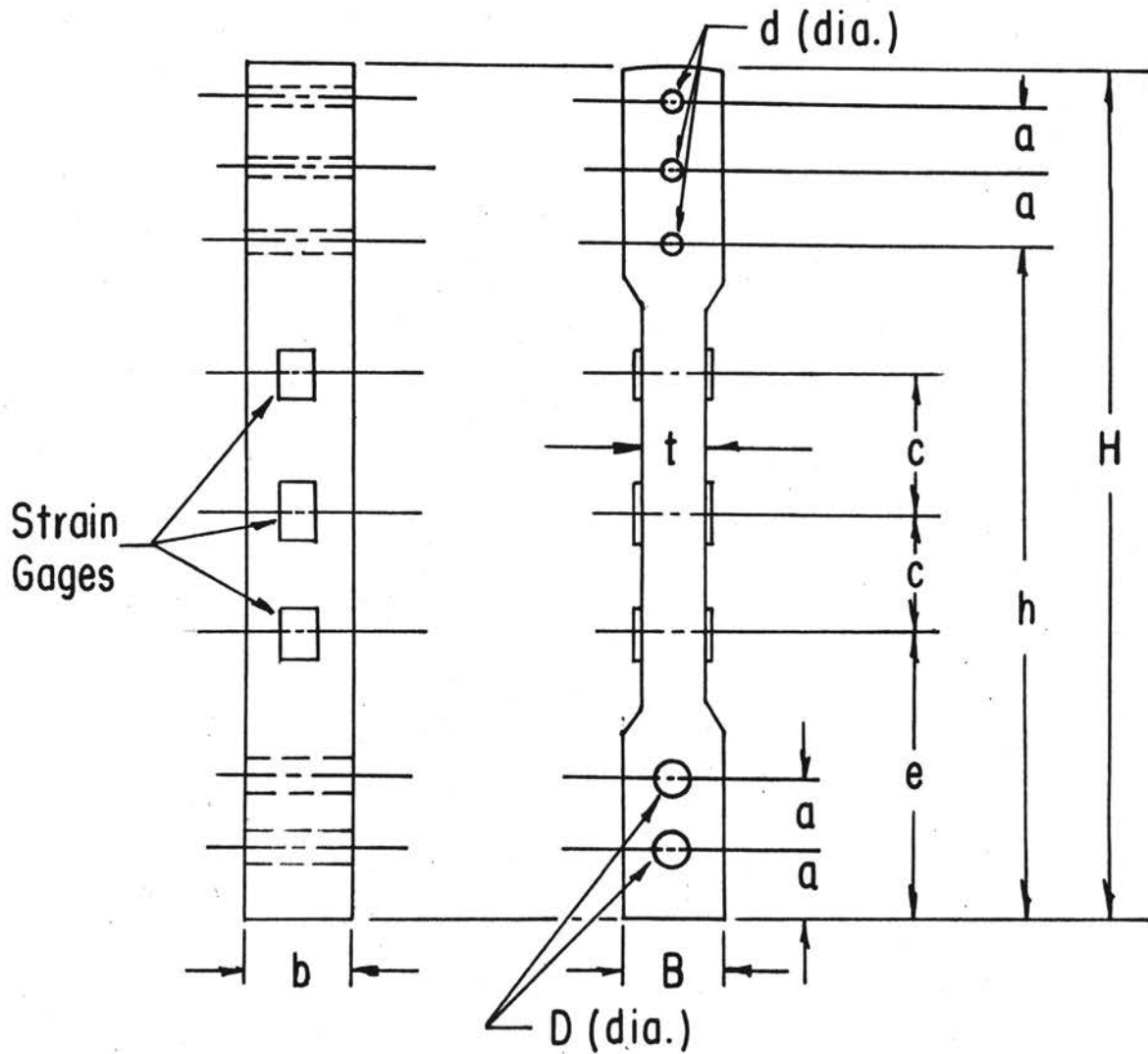
One of the eight foot floor sections located approximately at the center of the tunnel test section was removed and a special floor section installed in its place. The special floor section was used to prevent destruction of the original floor section and to facilitate installation of the model components.

The model roof components were supported with two mast supports. The supports were located 16 in apart for all of the tests with the exception of the shortest model. For the shortest model the mast supports were located 12 in apart. The mast supports were anchored to the tunnel floor with small steel brackets as shown in figure 9 so that the



No.	Type	Material	W in.	l in.
1	Solid	one inch lumber	48	$2\frac{1}{4}$
2	Solid	one inch lumber	48	3
3	Solid	one inch lumber	48	$4\frac{1}{2}$
4	Ventilated	wire mesh	48	$2\frac{1}{4}$
5	Ventilated	wire mesh	48	3
6	Ventilated	wire mesh	48	$4\frac{1}{2}$

Figure 7. Definition Sketch of Barrier



No.	No. Req'd	H in.	B in.	b in.	a in.	c in.	e in.	t in.	h in.	d in.	D in.
1	2	11 $\frac{1}{4}$	15/16	3/4	3/4	2	4	7/16	9 $\frac{1}{2}$	1/8	3/16
2	2	6-3/4	15/16	3/4	3/4	1	2 $\frac{1}{4}$	7/16	5	1/8	3/16

Figure 8. Definition Sketch of Model Mast Support

mast supports acted as simple cantilever beams.

Each mast support was shielded with a hollow cylindrical shield constructed of 26 gage galvanized sheet metal (figure 11) to prevent wind forces on the supports. Figure 10 illustrates the mast supports and the type of shield used.

At the base of each mast support a hole was drilled through the tunnel floor to provide a route for the wiring necessary for the force sensing devices.

Velocity Measuring Equipment

The wind tunnel was calibrated so that the speed at the test installation was measured by a static pressure piezometer ring located at the low pressure end of the wind tunnel. A precision manometer, figure 12, operating on the principle of a hook gage was used to obtain the static pressure readings. A graphical relationship between the static pressure at the static pressure piezometer ring and the velocity head at the test installation is represented in figure 13.

Apparatus For The Two-Dimensional Wind Profile

A device to generate a two-dimensional wind profile was constructed to investigate wind forces developed by it and compare these with the forces developed by a one-dimensional wind profile. The two-dimensional wind profile was only used with a system which had no upwind barrier, for it was thought that upwind barriers would so disrupt the flow of air that no useful information would be obtained in using the two-dimensional wind profile when upwind barriers were present.

The power law was selected to describe the variation of velocity

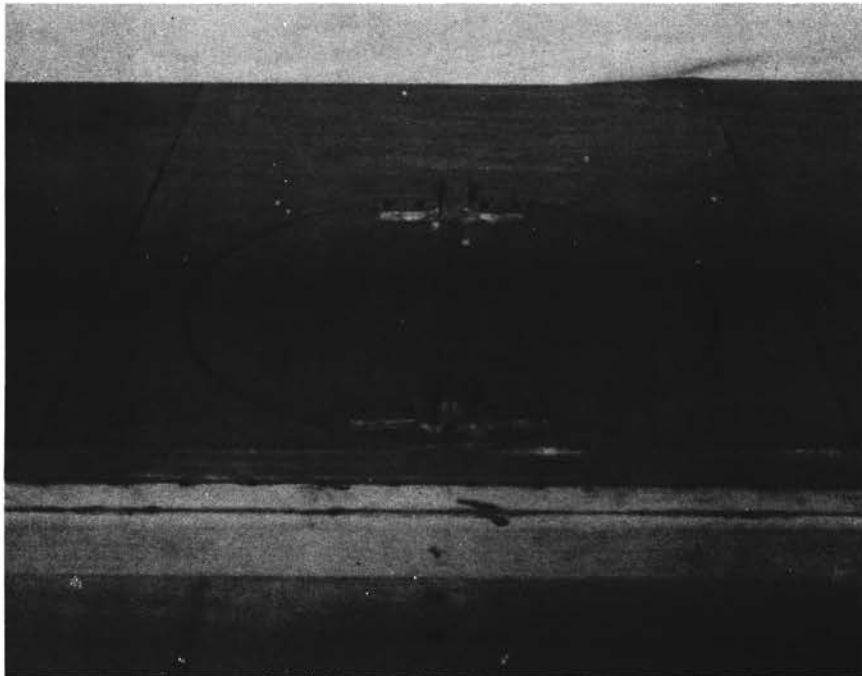


Figure 9. Anchors For Model Mast Supports

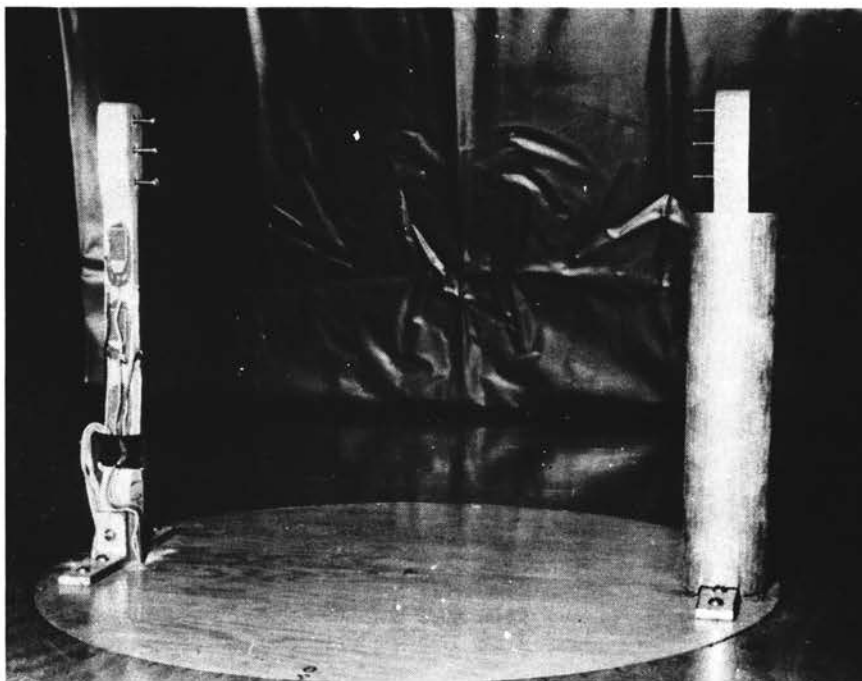
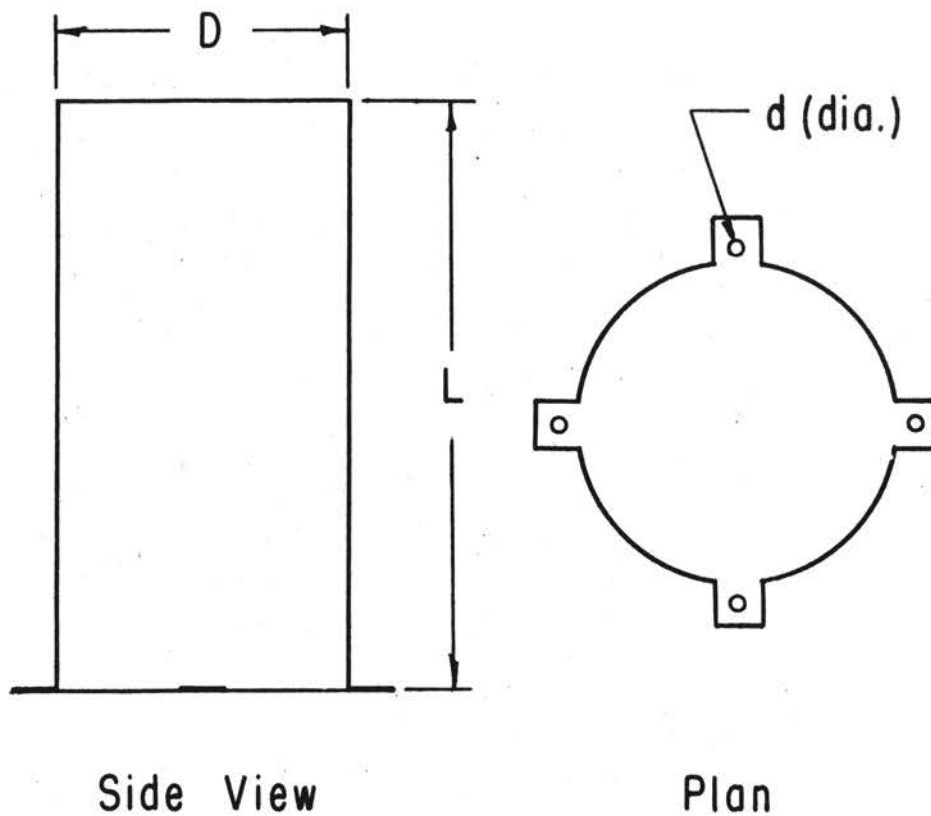


Figure 10. Mast Supports Installed In Wind Tunnel



Number Required	D in.	L in.	d in.
2	2	$4\frac{1}{4}$	1/8
2	2	$5\frac{1}{2}$	1/8
2	2	$8\frac{1}{2}$	1/8

Figure 11. Definition Sketch of Shield For Model Mast Support

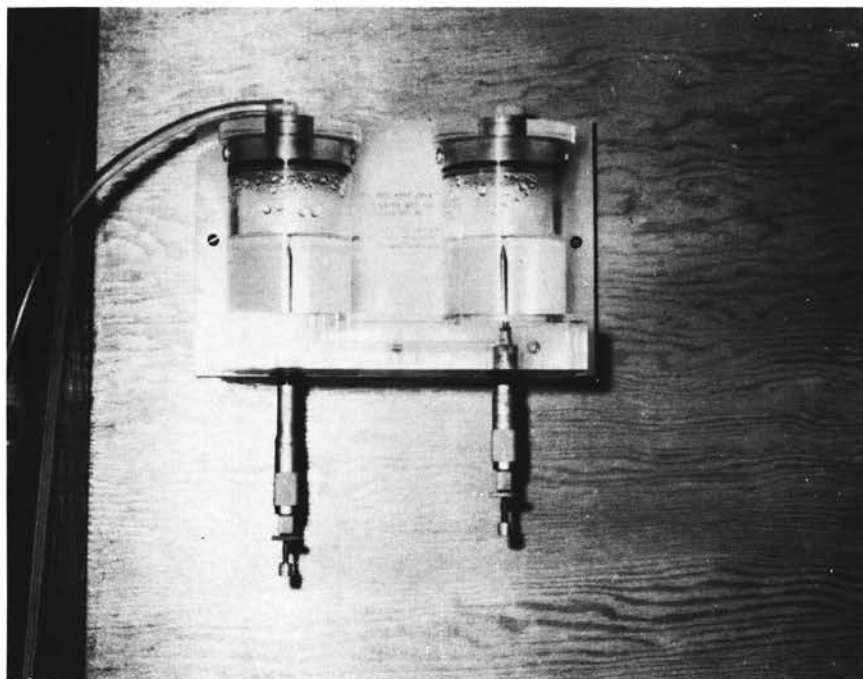


Figure 12. Precision Manometer Used For Obtaining The Static Pressures

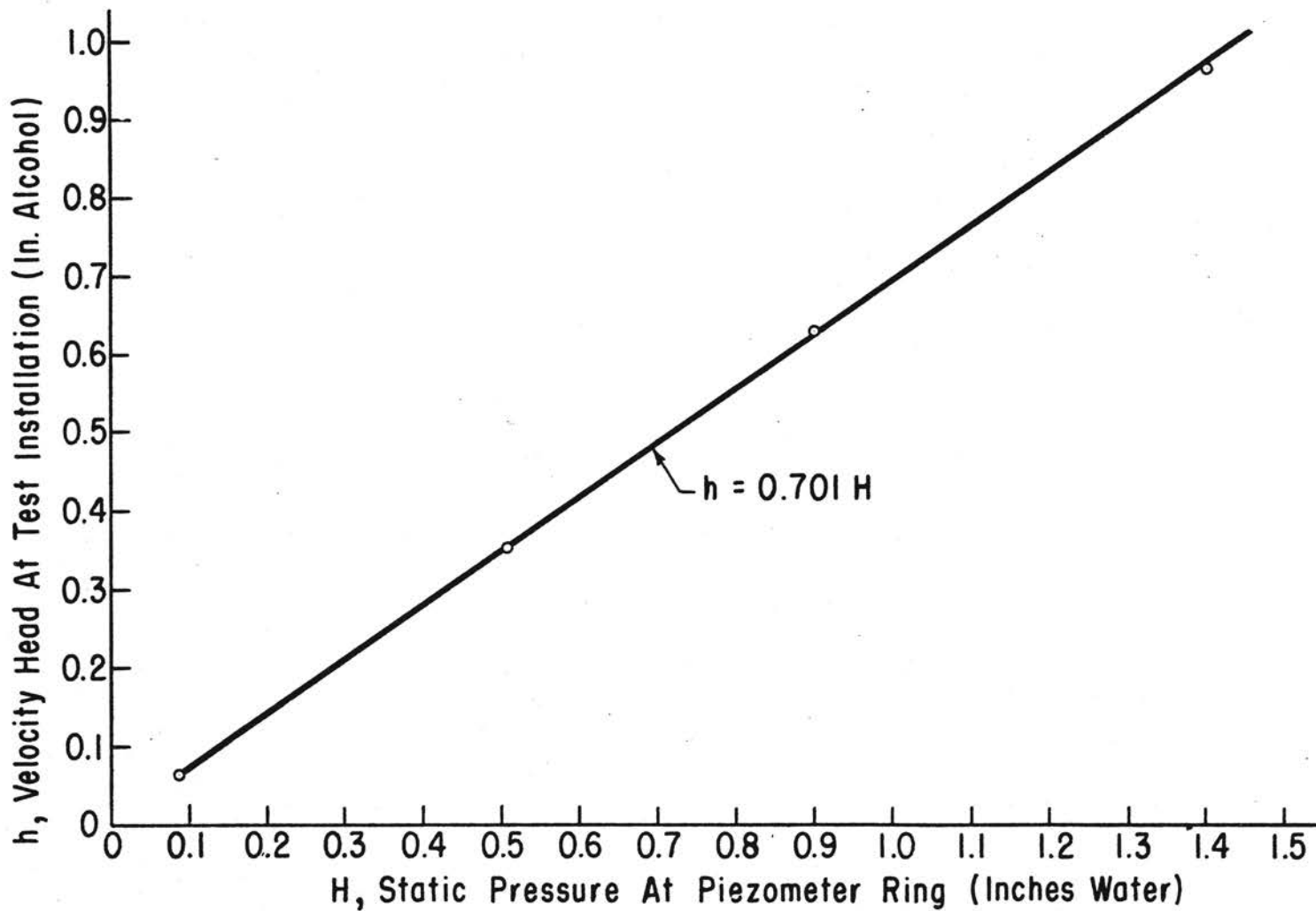


Figure 13. Relationship Between the Static Pressure and the Velocity Head at the Test Installation

with height. This law is

$$V/V_0 = (Z/Z_0)^\alpha$$

where, V = velocity at height Z ,
 V_0 = velocity at height Z_0 ,
 α = exponent.

The selection of an appropriate value for α is difficult, for there is no universal value recommended by all investigators. Many civil engineers recommend a value of $1/7$ for α for calculating the wind loads on tall structures such as skyscrapers. This value is probably a good assumption for these heights, but for heights below 20 or 30 feet, a value of α of $1/7$ does not seem appropriate. It would appear that the velocity profile closer to the ground would be steeper than the velocity profile at greater heights. Therefore, a value of $1/4$ was selected as the value of α for the present studies.

The desired velocity profile was obtained by a trial and error method of spacing rods of different diameters at various locations above the wind tunnel floor. The combination of rod sizes and spacings that gave the best profile is illustrated in figure 14.

A pitot-static tube and manometer with alcohol as the fluid was used to obtain the velocity head readings. Readings were taken 23 in downwind of the apparatus at heights of 2-1/2, 4, 6, 8, 10, 12, 16, 20, and 24 in above the tunnel floor. Readings were obtained at four different wind speeds. The 24 in elevation was used as the reference elevation.

The values V/V_0 versus Z/Z_0 were plotted on log-log paper to determine the goodness of fit for the different speeds. Figure 15 shows a plot of V/V_0 versus Z/Z_0 for a speed of 400 rpm. The slopes of the

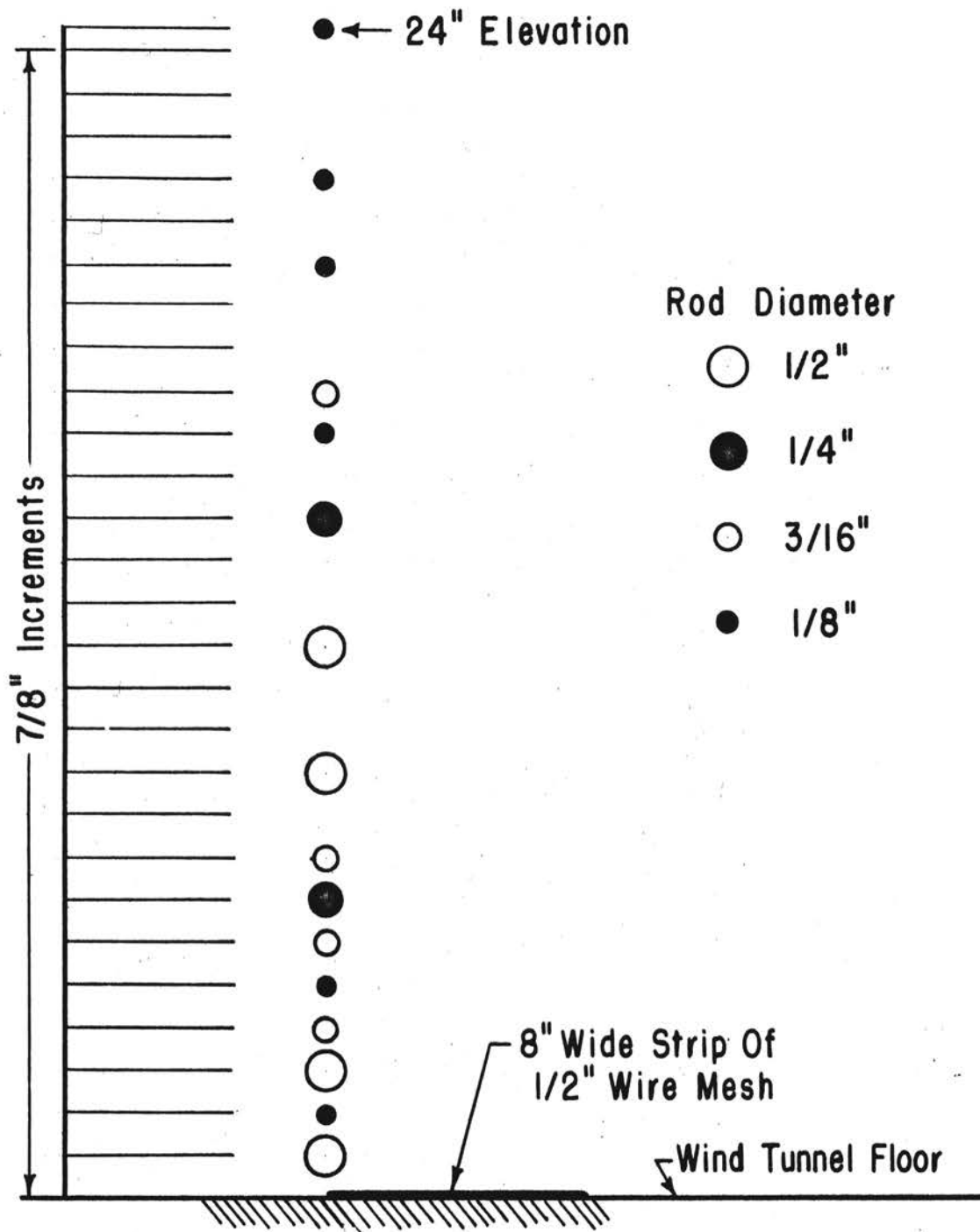


Figure 14. Size and Arrangement of Rods Used to Obtain the Two-Dimensional Wind Profile

velocity profiles were calculated using a linear regression analysis.

The values of the slopes from the linear regression analyses were:

rpm	slope = α
400	0.248825
500	0.249427
600	0.248869
700	0.254883

If these values of α are rounded off to two significant places each has a value of 0.25. Therefore, this profile was used and the value of α was assumed to be 0.25.

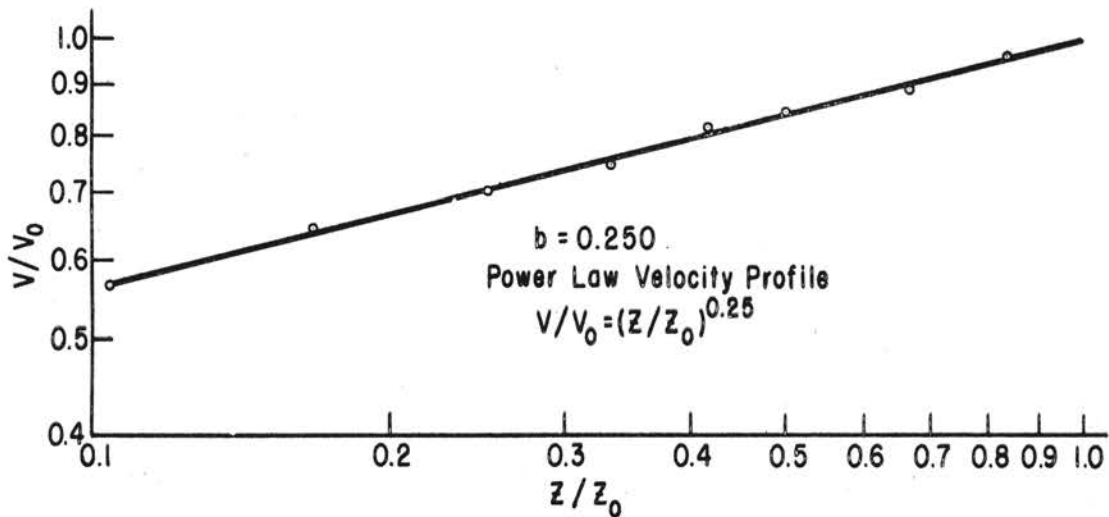


Figure 15. Slope of the Two-Dimensional Wind Profile on Log-Log Paper

CHAPTER V

PROCEDURE

Determination of the Velocity Distribution in the Wind Tunnel

A velocity traverse was made on a six-inch grid spacing across the wind tunnel, starting three inches from the tunnel walls, to determine the velocity distribution in the cross section of the tunnel. The equipment and instruments used were:

1. wind tunnel,
2. piezometer ring with manometer,
3. pitot-static tube with manometer,
4. barometer,
5. hygrothermograph,
6. thermocouple and potentiometer,
7. model of an umbrella shelter.

The model was placed in the position in the tunnel it was to occupy for the model study. The pitot-static tube was used to measure the velocity head in the tunnel and was placed approximately 10 ft upwind from the model. Barometric pressure readings were found with the barometer, relative humidity readings were found with the hygrothermograph, and tunnel air temperatures were found with the thermocouple and potentiometer. The piezometer ring, located at the low pressure end of the tunnel, was used to measure the static pressure readings. These were used to obtain a relationship between the static pressure at the piezometer ring and the velocity head readings at the test installation.

With the model installed readings were taken at each station in the cross section of the tunnel at four different wind speeds. With the grid spacing used there were 64 stations in the cross section of

the tunnel.

The results revealed a fairly uniform velocity distribution in the cross section of the tunnel with the exception of the corner positions. The velocity variation in the cross section of the tunnel was found to have a standard deviation of approximately 2.8 per cent. The relationship between the velocity head readings at the test installation and the static pressure readings is shown in figure 13.

General Procedure For Conducting Experiments

1. The proper model installation was made in the wind tunnel. The parameter combinations for the individual experiments are tabulated in table II. Figure 16 shows a typical model installation in the wind tunnel.

2. The strain gage circuits were balanced using the bridge balancing unit and the strain indicator. The bridge balancing unit and strain indicator are illustrated in figure 17.

3. The precision manometer at the static pressure piezometer ring was adjusted and the zero readings obtained. The precision manometer is illustrated in figure 12.

4. The wind tunnel was started and the air was allowed to recirculate through the laboratory space for approximately 10 minutes in order for the laboratory air to reach a fairly constant temperature.

5. Barometric pressure and relative humidity readings were obtained at the start of each experiment. As each individual experiment took only about 30 minutes, these readings were taken only once during each experiment.

6. The wind speed was adjusted to a selected value using the RPM indicator. The experiments were conducted at four different wind speeds.

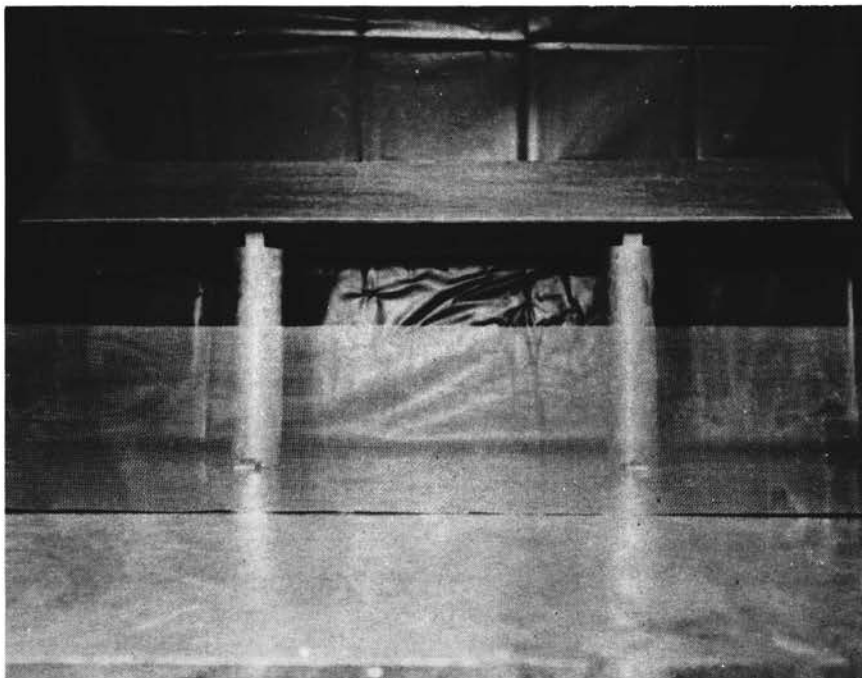


Figure 16. Model Installation In Wind Tunnel

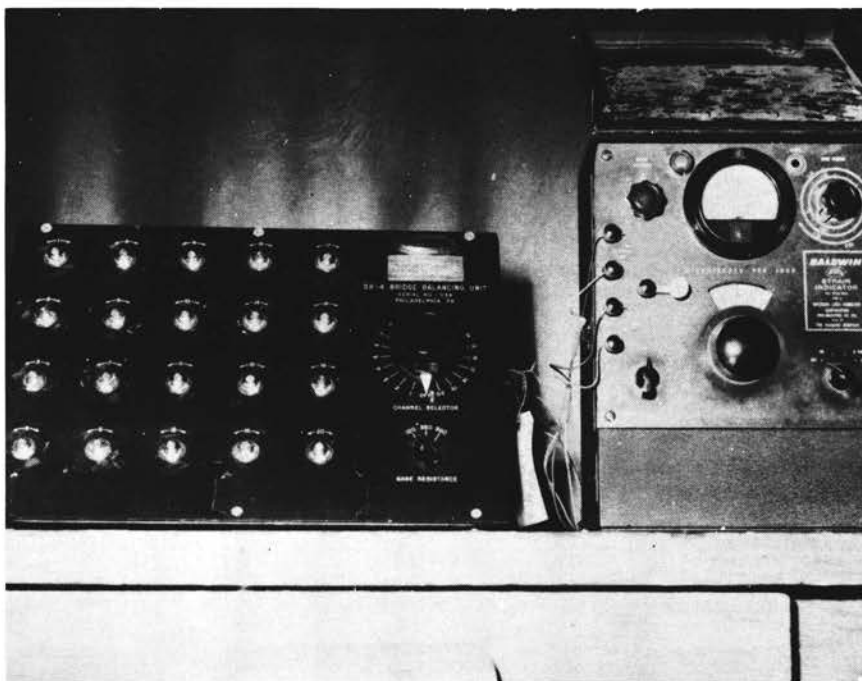


Figure 17. Bridge Balancing Unit and Strain Indicator
Used For Measuring Strain

At each wind speed the following readings were obtained:

- (a). Strain reading for each gage pair. As vibration of the model caused unsteadiness of the strain indicator needle, three replications of the strain readings were recorded.
- (b). Tunnel air temperature readings.
- (c). Static pressure readings at the static pressure piezometer ring.

For the tests using the two-dimensional flow pattern, the wind profile generating apparatus was installed approximately 24 inches upwind of the model installation. The same general procedure as has been outlined above was followed for these tests with the exception of obtaining the velocity head readings. These were obtained with pitot-static tube located 24 inches above the tunnel floor, and approximately 24 inches downwind of the profile apparatus. The pitot-static tube was even with the leading edge of the model and 12 in above the ridge of the model.

CHAPTER VI

ANALYSIS OF DATA

Calculation of Wind Velocities

The velocity head at the test installation was found from the static pressure readings and the relationship between the static pressure reading and the velocity head at the test installation, figure 13. The velocity heads at the test installation were measured by manometer readings. Therefore, these readings had to be converted to ft of air. The following procedure was followed for calculating the velocities.

$$V = \sqrt{2gH}$$

where, V = velocity at the test section in ft/sec,

$$g = 32.2 \text{ ft/sec}^2,$$

H = velocity head in ft of air, measured with a pitot-static tube.

Then:

$$H = (h)(\rho_A)/(12)(\rho_a)$$

where, h = velocity head reading in inches of alcohol,

$$\rho_A = \text{density of alcohol} = 49.42 \text{ lb}_m/\text{ft}^3,$$

$$\rho_a = \text{density of air in lb}_m/\text{ft}^3,$$

12 was used to convert the inches of alcohol to feet of alcohol.

Then:

$$H = (49.42)(h)/(12)(\rho_a) = 4.118(h)/\rho_a.$$

Substitute H into $V = \sqrt{2gH}$

$$V = \sqrt{(2)(32.2)(4.118) h/\rho_a} = 16.28 \sqrt{h/\rho_a}.$$

Calculation of π_g Parameters

Using the observed strain readings obtained from the experiments the corresponding bending moments for each gage location and speed were found from the calibrations relating strain to bending moment. The average moment of the two mast supports was used for the analysis.

The average moment at each gage location and each speed was plotted against the gage location along the mast support. A plot of this type was made for each test. It was known from elementary mechanics that the moment varied linearly along the mast. Therefore, a straight line was fitted to the plot of observed moments to define the moment diagram for the mast support. The intersection of this moment diagram with the mast axis established the point of zero bending moment in the mast support. From the plots, the value of y , the distance measured downward from the eave to the point of zero bending moment in the mast, was found. Figure 18 shows a typical plot of the bending moment diagram. With the y values known, the $\pi_g = y/Z$ values were then calculated. These values are tabulated in appendix A.

Calculation of π_q Parameters

After the bending moment for each gage location and each speed had been established, the shear, H , in the mast support was found for each speed using the relation $H = \Delta M / \Delta x$, where ΔM is the change in bending moment in the distance Δx .

The shear H was then plotted against the corresponding velocity squared V^2 . A linear relationship existed between H and V^2 for each of the model tests. Figure 19 shows a typical plot of H versus V^2 . The

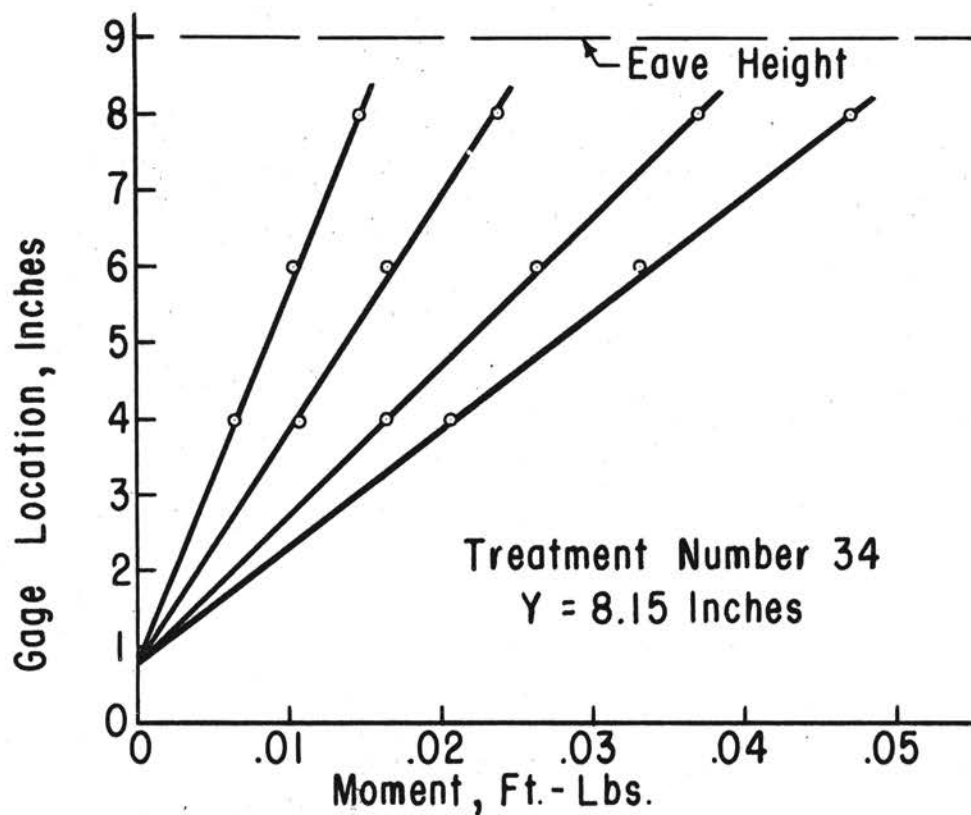


Figure 18. Typical Moment Diagram for the Model Mast Support

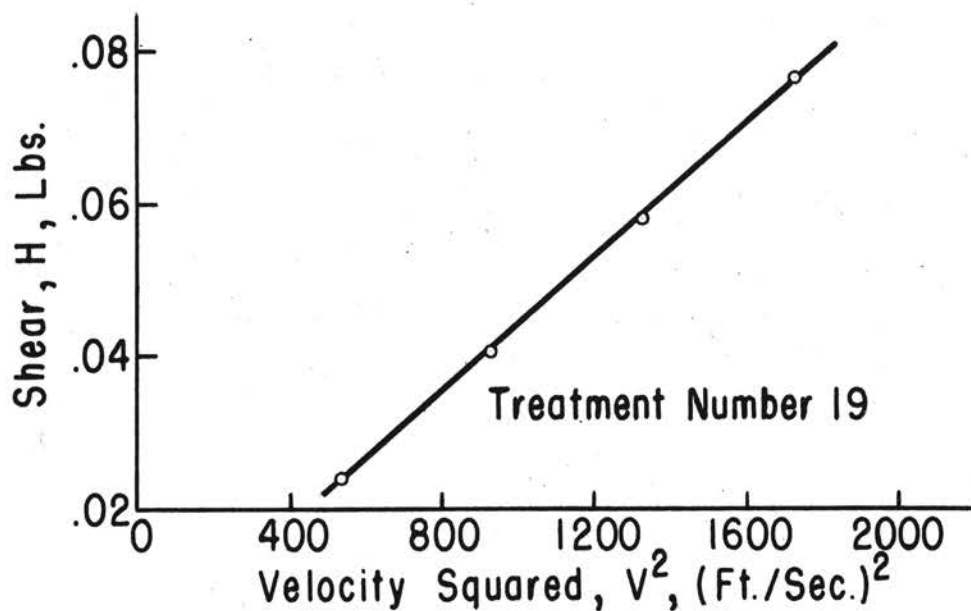


Figure 19. Typical Plot of the Shear Versus the Velocity Squared

slope H/V^2 was then found and this value used to calculate the π_q values, equal to $2H/kDW\rho V^2$. These values are tabulated in appendix A.

Statistical Analyses

Statistical analyses of variance, as outlined by Snedecor (20, chap. 12), were applied to the data obtained from the experiments. The variance ratios and significance levels were calculated for π_g and π_q . The combination of parameter values for each of the various analyses are tabulated in table III. The variance ratios and significance levels for differences in π_g are summarized in table IV and for differences in π_q in table V. The individual analysis of variance tables are presented in appendix B.

TABLE III
PARAMETER COMBINATIONS FOR THE STATISTICAL ANALYSES

Parameter	Analysis 1	Analysis 2	Analysis 3	Analysis 4
π_1	0.3846	0.2425	0.2425	0.2425
		0.3846	0.3846	0.3846
		0.5187	0.5187	0.5187
π_2	$\frac{1}{3}$	$\frac{1}{3}$	$\frac{1}{3}$	$\frac{1}{3}$
		$\frac{2}{3}$	$\frac{2}{3}$	$\frac{2}{3}$
π_3	$\frac{1}{6}$	$\frac{1}{10}$	$\frac{1}{10}$	$\frac{1}{10}$
	$\frac{1}{10}$			
	$\frac{1}{12}$			
	$\frac{1}{18}$			
π_4	2		2	
	6		6	
π_5	$\frac{1}{2}$	No Barriers	$\frac{1}{2}$	
π_6	0		0	
	.50		.50	
Barrier Type				Absent Solid Ventilated

TABLE IV

SUMMARY TABLE OF THE VARIANCE RATIOS AND SIGNIFICANCE LEVELS
ASSOCIATED WITH DIFFERENCES IN π_B , THE PARAMETER
DEFINING THE LOCATION OF ZERO BENDING MOMENT

Parameter	Analysis 1		Analysis 2		Analysis 3		Analysis 4	
	Var. Ratio	Sign. Level	Var. Ratio	Sign. Level	Var. Ratio	Sign. Level	Var. Ratio	Sign. Level
π_1 , Roof Slope			13,181.5	>99.95	29.2538	>99.95	95.0993	>99.95
π_2 , Shelter Height			11,145.2	>99.95	31.1613	>99.95	96.5774	>99.95
π_3 , Shelter Length	18.7536	>99.95						
π_4 , Barrier Spacing	7.2076	>99.95			0.5311			
π_6 , Barrier Ventilation	1,1286	70.23			2.2006	79.20		
Comparison Of Solid Barrier Ventilated Barrier No Barrier							3.6426	95.00

TABLE V

SUMMARY TABLE OF THE VARIANCE RATIOS AND SIGNIFICANCE LEVELS
ASSOCIATED WITH DIFFERENCES IN π_q , THE WIND FORCE PARAMETER

Parameter	Analysis 1		Analysis 2		Analysis 3		Analysis 4	
	Var. Ratio	Sign. Level	Var. Ratio	Sign. Level	Var. Ratio	Sign. Level	Var. Ratio	Sign. Level
π_1 Roof Slope Parameter			3.5961	92.88	5.3305	96.85	93.9424	>99.95
π_2 Shelter Height Parameter			10.1710	99.03	1.1260	67.78	6.2314	99.07
π_3 Shelter Length Parameter	12.4032	>99.95						
π_4 Barrier Spacing Parameter	0.8480				11.5961	99.17		
π_6 Barrier Ventilation Parameter	0.7327				14.4258	99.54		
Comparison Of Solid Barrier Ventilated Barrier No Barrier							231.14	>99.95

CHAPTER VII

DISCUSSION OF RESULTS

The objective of the present study was to evaluate the gross horizontal and overturning wind forces on open or umbrella-type shelters as influenced by shelter length, shelter height, roof slope, and upwind barriers. To completely define the horizontal and overturning wind forces on open or umbrella-type shelters the total horizontal force and the point of zero bending moment along the axis of the masts must be known. The two dependent parameters π_B and π_q are measures of these values. These parameters were evaluated for each of the individual tests and the values tabulated in appendix A.

A value of π_B equal to one corresponds to a location of zero bending moment in the masts at the ground surface. The values of π_B reveal that the bending moment in the masts was usually zero near the ground surface. This was in contrast to the results that would be obtained in using the concept of a unit pressure applied to the vertical projection of the roof. This concept would produce a calculated maximum moment at the ground surface; whereas in reality the maximum moment usually occurred at the eaves level.

The π_q parameter, equal to $2H/kDW \ominus V^2$, is an index of the total horizontal force on a shelter, for $2H$ equals the total horizontal force on the shelter. Therefore, the smaller the π_q value for a given shelter configuration, the smaller the horizontal force on the shelter. For instance, for a given shelter configuration under identical con-

ditions, a π_q value equal to 0.60 would correspond to horizontal force on the shelter twice as large as a π_q value equal to 0.30.

Statistical Analyses

A study of table IV reveals that the variance ratios associated with differences in π_g due to the barrier parameters were appreciably smaller than the variance ratios associated with differences in π_g due to differences in the roof slope, shelter height, and shelter length parameters. For instance, for analysis 3, table IV, the variance ratios associated with differences in π_g due to differences in the roof slope and shelter height parameters were 29.3 and 31.2 respectively with a significance level greater than 99.95 for each; but the variance ratios associated with differences in π_g due to differences in barrier spacing and barrier ventilation parameters were only 0.53 and 2.2 respectively.

The variance ratios associated with differences in π_q , table V, due to the roof slope and shelter height parameters were smaller than the variance ratios associated with differences in π_q due to differences in the shelter length and barrier parameters.

A summary of the mean values of π_g and π_q is tabulated in table VI for the different treatments.

Effect of Roof Slope

The roof slope parameter had a very strong effect on the values of π_g . From table VI, the mean π_g values for the 3/12, 5/12, and 7/12 roof slopes were 2.4440, 1.3222, and 0.6967 respectively. The π_g value for the 5/12 roof slope was approximately twice the π_g

TABLE VI

MEAN VALUES FOR π_8 , THE PARAMETER DEFINING THE LOCATION OF ZERO BENDING MOMENT, AND π_9 , THE WIND FORCE PARAMETER

EFFECT	TREATMENT	π_8	π_9
ROOF SLOPE	$\pi_1 = 0.2425$	2.4440	0.4551
	$\pi_1 = 0.3846$	1.3222	0.5532
	$\pi_1 = 0.5187$	0.6967	0.5497
SHELTER HEIGHT	$\pi_2 = \frac{1}{3}$	1.0029	0.5240
	$\pi_2 = \frac{2}{3}$	2.0257	0.5065
SHELTER LENGTH	$\pi_3 = \frac{1}{6}$	0.9029	0.3337
	$\pi_3 = \frac{1}{10}$	0.9073	0.5754
	$\pi_3 = \frac{1}{12}$	1.0213	0.4620
	$\pi_3 = \frac{1}{18}$	1.0225	0.5063
BARRIER SPACING	$\pi_4 = 2$	1.5313	0.4428
	$\pi_4 = 6$	1.4102	0.5647
BARRIER VENTILATION	$\pi_6 = 0$	1.3476	0.4373
	$\pi_6 = .50$	1.5939	0.5738
BARRIER	ABSENT	1.6886	0.6067
	SOLID	1.3476	0.4373
	VENTILATED	1.5939	0.5738

value for the 7/12 roof slope and the π_g value for the 3/12 roof slope was approximately twice the π_g value for the 5/12 roof slope and approximately 4 times the π_g value for the 7/12 roof slope. Thus, for a 3/12 roof slope, the point of zero bending moment was approximately twice as far below the eaves as for the 5/12 roof slope, and approximately 4 times as far below the eaves as for the 7/12 roof slope.

The roof slope had very little effect on the values of π_q for cases in which no upwind barriers were present. For a system with $\pi_3 = 1/10$, $\pi_2 = 1/3$, and no upwind barriers, the π_q values for the 3/12, 5/12, and 7/12 roof slopes were 0.6470, 0.6377, and 0.6075 respectively. The greatest variation in the three values was 6.2 per cent with the lowest π_q value associated with the 7/12 roof slope. For cases with an upwind barrier there was very little difference between the π_q values associated with the 5/12 and 7/12 roof slopes. However, the π_q values associated with the 3/12 roof slope with an upwind barrier were approximately 20 per cent smaller than the π_q values for the 5/12 and 7/12 roof slopes with an upwind barrier.

Effect of Shelter Height

The model experiments were conducted at two shelter heights, corresponding to π_2 values of 1/3 and 2/3. From table VI, a comparison of the mean values of π_g for the shelter height treatments, reveals that the mean value of π_g with $\pi_2 = 2/3$ was 202 per cent of the mean value of π_g with $\pi_2 = 1/3$. This means that for a given eaves height the point of zero bending moment along the axis of the masts was approximately twice the distance from the eaves for $\pi_2 = 2/3$ compared to $\pi_2 = 1/3$.

Changes in shelter height had very little effect on the π_q values. The mean π_q values, table VI, equal to 0.5240 and 0.5065 for $\pi_2 = 1/3$ and $\pi_2 = 2/3$ respectively differed by less than four per cent.

Effect of Shelter Length

No appreciable variation was found to exist between π_g values for changes in shelter length.

The π_q values varied appreciably with changes in shelter length. The mean values of π_q were 0.3337, 0.5754, 0.4620, and 0.5063 corresponding to π_3 values of 1/6, 1/10, 1/12, and 1/18 respectively. The smallest π_q value of 0.2308 was associated with $\pi_3 = 1/6$. This represents the shortest shelter length. This small value of π_q associated with the shortest shelter can probably be attributed to the effect of end flow around the model. Relatively more flow occurred around the ends of the shorter models, thereby reducing the total horizontal force on the shelter.

Effect of Upwind Barriers

Two types of upwind barriers were used in the model study; a solid, and a ventilated barrier having a uniformly distributed open area of approximately 50 per cent of the gross area.

For a given shelter configuration it was found that the π_g value was usually greater for a ventilated barrier compared to a solid barrier. For a given eaves height and barrier spacing, the value of π_g averaged approximately 15 per cent greater for a ventilated barrier compared to a solid barrier.

The π_q values associated with a solid upwind barrier were ap-

preciably smaller than the π_q values associated with a ventilated upwind barrier. The π_q values associated with a solid upwind barrier averaged 23.8 per cent less than the π_q values associated with a ventilated upwind barrier. This means that a solid barrier was more effective than a ventilated barrier in reducing the wind forces on open or umbrella-type shelters. The reduction in the π_q values associated with a solid upwind barrier was dependent upon the spacing between the shelter and the barrier. The π_q values associated with a ventilated upwind barrier were in general independent of the barrier spacing.

Two barrier spacings, corresponding to π_4 values of two and six, were used for each shelter configuration. For one shelter configuration, 5/12 roof slope, $\pi_3 = 1/10$, $\pi_5 = 1/2$, and $\pi_2 = 1/3$, nine barrier spacings were used to study more completely the effect of barrier spacing on the π_8 and π_q parameters.

The π_8 parameter did not change appreciably with changes in barrier spacing. Figures 20 and 21 show graphical representations of π_8 as a function of π_4 and also give the corresponding linear regression equations.

Changes in upwind spacing of solid barriers were found to have a very pronounced effect on the π_q values, as shown in figure 23. From figure 23 it is seen that as the barrier spacing was increased, the π_q value also increased. This indicates that the solid barriers close to the shelter were more effective in reducing the wind forces on the shelter.

Figure 22 shows π_q as a function of π_4 for a ventilated upwind barrier. It appeared that the π_q values were independent of the ventilated barrier spacing.

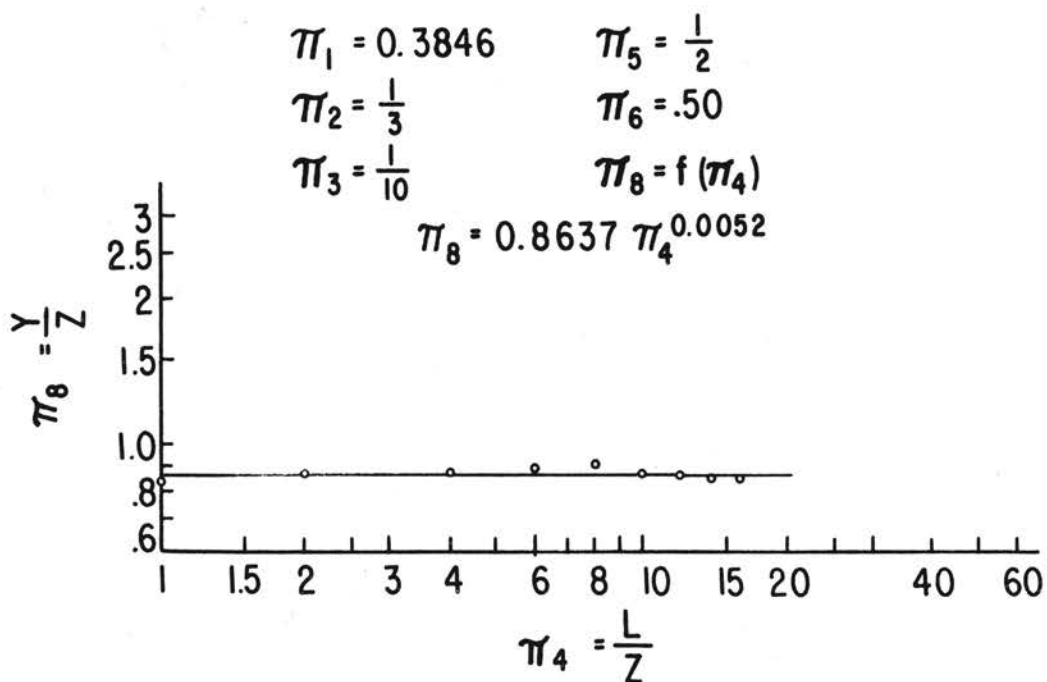


Figure 20. π_8 as a Function of π_4 for a Ventilated Barrier

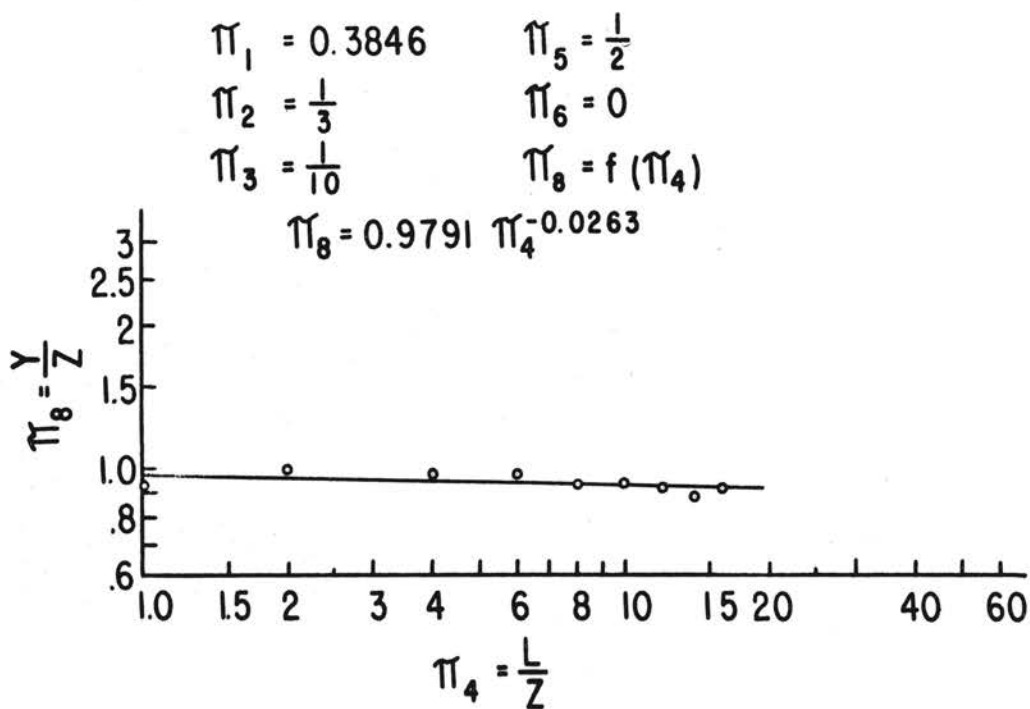


Figure 21. π_8 as a Function of π_4 for a Solid Barrier

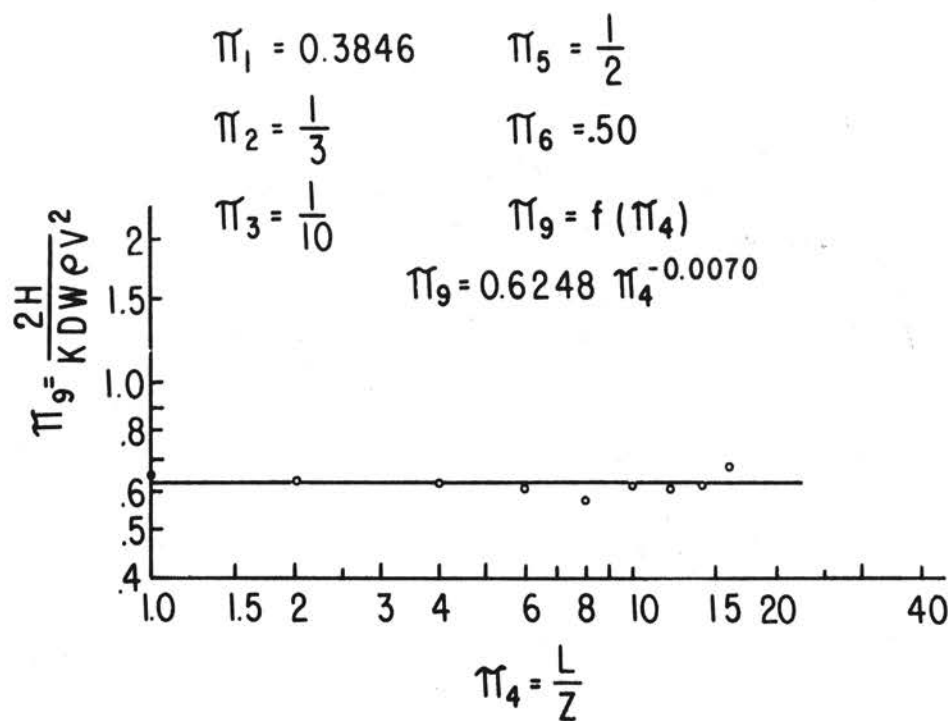


Figure 22. π_9 as a Function of π_4 for a Ventilated Barrier

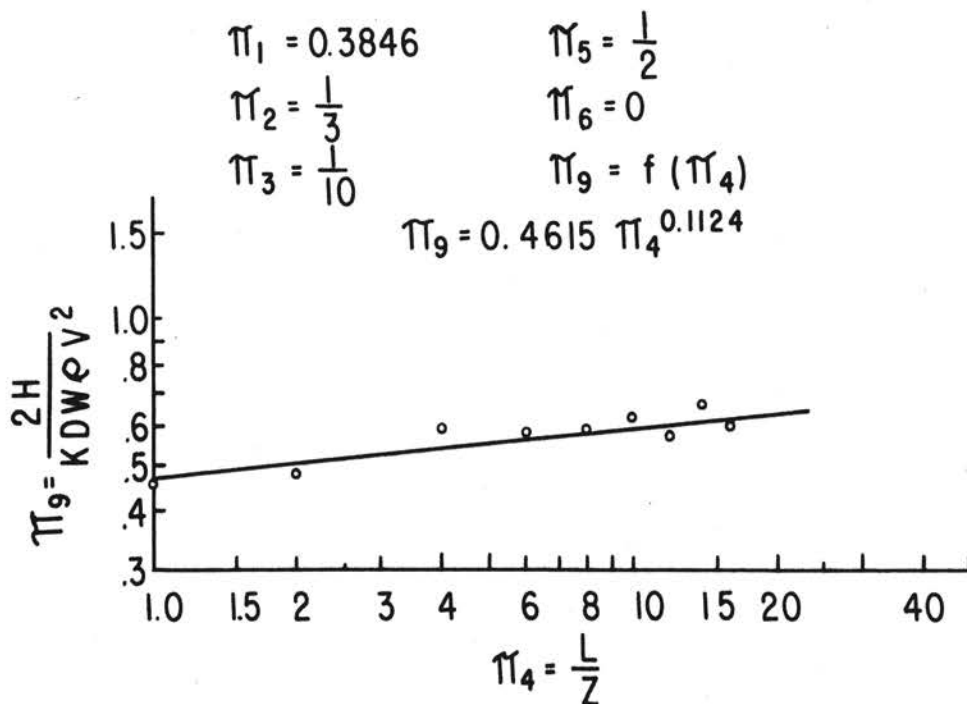


Figure 23. π_9 as a Function of π_4 for a Solid Barrier

Reynolds Number

The range of Reynolds numbers for the model experiments varied from approximately 25,000 to 60,000. The Reynolds numbers are tabulated in appendix A. The length factor used in the Reynolds number was the projected height of the shelter, eaves to ridge.

Four different wind speeds were used to evaluate π_q for each treatment combination. Analysis of the data revealed that π_q , a wind force coefficient, was independent of Reynolds number in the range of velocities used for the study. These results support the conclusion of some investigators that the results obtained from model studies on sharp-edged bodies can be transferred to any larger scale regardless of the velocity.

Comparison of One-Dimensional and Two-Dimensional Velocity Profiles

A two-dimensional velocity profile described by the power law was used with a 3/12, 5/12, and 7/12 roof slope with $\pi_3 = 1/10$, $\pi_2 = 1/3$, and no upwind barriers to determine the effect of wind gradient on the π_g and π_q parameters. The velocity head for the one-dimensional flow pattern was measured at the static pressure piezometer ring located at the low pressure end of the wind tunnel. This velocity head is the average velocity head occurring at the test installation. The velocity head for the two-dimensional flow pattern was measured with a pitot-static tube located 24 inches downwind from the device used to generate the two-dimensional flow pattern. The pitot-static tube was 12 inches above the ridge and at the leading edge of the model. The velocity head used was the average effective velocity head occurring in

the zone from the lower edge of the eaves to the ridge of the model.

TABLE VII
COMPARISON OF THE π_b AND π_q VALUES OBTAINED
WITH A ONE-DIMENSIONAL WIND PROFILE AND
A TWO-DIMENSIONAL WIND PROFILE

Roof Slope	π_b		π_q	
	One-Dimensional Wind Profile	Two-Dimensional Wind Profile	One-Dimensional Wind Profile	Two-Dimensional Wind Profile
3/12	1.7458	1.6556	0.6470	0.5190
5/12	0.8089	0.8100	0.6377	0.6589
7/12	0.4022	0.4178	0.6075	0.6496

From table VII it was found that there was very little difference between the π_b values for the two profiles. Comparing the π_q values for the two profiles, table VII, it was found that there was very little difference between the π_q values for the 5/12 and 7/12 roof slopes. However, for the 3/12 roof slope the π_q value associated with the two-dimensional velocity profile was 19.5 per cent smaller than the π_q value associated with the one-dimensional velocity profile.

Comparison of π_q as Found by; Present Data,
ARS Data, and Irminger and Nøkkentved's Data

Table VIII gives a comparison of the π_q values obtained with, the present experimental data, ARS data (28, pp. 1-4) and Irminger and Nøkkentved's data (10, pp.64-65), respectively. The ARS data and the Irminger and Nøkkentved data are based on the average distribution in terms of the velocity pressure, $q = k \rho V^2/2$, on the roofs. The average distributions in terms of the velocity pressure q on the roofs as given by the ARS (28, p. 4, table 4) are

Windward Roof

0 to 20° slope	0.77 q - suction
20 to 30° slope	0.77 q to 0 - suction
30 to 60° slope	0 to 0.58 q - pressure

Leeward Roof

any slope	0.58 q - suction
-----------	------------------

These values are based on windtight buildings. The ARS (28, p.4) suggested adding 0.77q pressure out on roofs for buildings with 30 per cent or more wall openings in the windward wall, and adding 0.58q suction in on roofs for buildings having 30 per cent or more openings in the leeward wall. If both the leeward and windward walls have 30 per cent of more wall openings, this would suggest adding the difference between 0.77q pressure out and 0.58q suction in to the roofs. The net result would be addition of 0.19q pressure outward on the roofs.

Irminger and Nøkkentved gave results for a 30° roof slope only. The average pressures in terms of the velocity pressure q on the roofs as given by Irminger and Nøkkentved (10, p. 64) are

Windward Roof	0.72q - pressure
Leeward Roof	0.35q - suction

Irminger and Nøkkentved's data were obtained by experiments on open shed models in a wind tunnel. The roofs of the models were made of double plates with a space between, making it possible to measure the pressure distribution on both the upper and lower roof surfaces.

The present experimental models had slopes of 3/12, 5/12, and 7/12, corresponding to slope angles of 14.05°, 22.63°, and 30.25° respectively.

The total horizontal force on an umbrella shelter using the average distribution method is:

$$2H = (n)(k \rho V^2/2)(W)(D/\sin \theta)(\sin \theta) \quad (a)$$

where, $2H$ = total horizontal force on shelter, lbf ,

n = surface-average pressure coefficient from ARS or Irminger and Nøkkentved data, dimensionless,

$k \rho V^2/2$ = velocity pressure, lbf/ft^2 ,

W = shelter length, ft ,

$D/\sin \theta$ = roof slope length, ft ,

θ = slope angle.

The values of $\pi_q = 2H/kDW \rho V^2$ were calculated for both sets of data (ARS, Irminger and Nøkkentved) using equation (a). The results are presented in table VIII and compared with the π_q values obtained experimentally in the present study.

TABLE VIII

COMPARISON OF π_q VALUES, THE WIND FORCE PARAMETER, OBTAINED WITH: PRESENT EXPERIMENTAL DATA, ARS DATA AND IRMINGER AND NØKKENTVED'S DATA

Roof Slope	Present Study	ARS Data	Irminger and Nøkkentved's Data
3/12	0.4551	0.0950	-
5/12	0.5532	0.0000	-
7/12	0.5497	0.2900	0.5350

From table VIII it is found that the calculated π_q values using the ARS data were much smaller than the π_q values found by the other two methods. For the 5/12 roof slope, using the ARS data, the average pressure distribution on the windward and leeward roofs are equal in character and magnitude, resulting in no horizontal shear. Good agreement exists between the π_q values obtained by the present

experiments and by Irminger and Nøkkentved.

The results from table VIII indicate that wind pressure data obtained from experiments conducted on windtight buildings are not applicable to open or umbrella-type shelters.

Application of Experimental Results

The results obtained from this experimental study may be used directly in the design of structural masts for open or umbrella-type shelters provided that the prototype is similar to one of the models in the present study. An example is given below demonstrating how the experimental results may be used to determine the horizontal and overturning wind forces on a typical umbrella shelter.

Consider an umbrella shelter, 50 ft in length, 5/12 roof slope, a 5 ft rise from eaves to ridge, and an eaves height of 15 ft.

Assumptions

1. No barriers or windbreaks in the general vicinity.
2. Wind velocity = 82 mph = approximately 120 ft/sec.
3. Mass density of air = $0.0760 \text{ lb}_m/\text{ft}^3$.

Corresponding to model nomenclature:

$D = 5 \text{ ft}$	$Q = 0.0760 \text{ lb}_m/\text{ft}^3$
$W = 50 \text{ ft}$	$k = 1/32.2 \text{ lb}_f/(\text{lb}_m\text{-ft}/\text{sec}^2)$
$Z = 15 \text{ ft}$	$L = - \text{ (no barrier)}$
$S = 13 \text{ ft}$	$l = - \text{ (no barrier)}$
$V = 120 \text{ ft}/\text{sec}$	$P = - \text{ (no barrier)}$

Then: $\pi_1 = D/S = 5/13 = 0.3846$

$$\pi_2 = D/Z = 5/15 = 1/3$$

$$\pi_3 = D/W = 5/50 = 1/10$$

These parameter values correspond to treatment number 16 for

which:

$$\pi_g = y/z = 0.8089 \quad (\text{appendix A})$$

Then, $y = 0.8089(z) = (0.8089)(15 \text{ ft}) = 12.13 \text{ ft}.$

y represents the location of zero bending moment measured downward from the eaves along the axis of the mast.

$$\text{Also, } \pi_q = 2H/kDW \rho V^2 = 0.6377 \quad (\text{appendix A})$$

where $2H$ represents the total horizontal force on the shelter.

$$2H = 1/32.2 \text{ lb}_f / (\text{lb}_m\text{-ft}/\text{sec}^2) (5 \text{ ft}) (50 \text{ ft}) (0.0760 \text{ lb}_m/\text{ft}^3) \\ (120 \text{ ft}/\text{sec})^2 (0.6377)$$

$$2H = 5,415 \text{ lb}_f$$

Maximum moment = $(12.13 \text{ ft})(5,415 \text{ lb}_f) = 65,683 \text{ ft-lb}_f.$ This maximum moment occurs at the eaves level.

Moment at the ground = $(-2.87 \text{ ft})(5,415 \text{ lb}_f) = -15,541 \text{ ft-lb}_f.$ This moment at the ground is negative, or opposite to the moment at the top of the mast.

Suppose the shelter has masts 10 ft o. c. along its length, making five bays. The forces on each bay would then be:

$$\text{Moment at top of mast} = 13,137 \text{ ft-lb}_f,$$

$$\text{Moment at ground} = -3,108 \text{ ft-lb}_f,$$

$$\text{Horizontal shear} = 1,083 \text{ lb}_f.$$

Oscillatory Forces

During the experiments an oscillatory force effect was noted on the model shelters. This oscillatory force effect was more pronounced with a solid upwind barrier as compared to no upwind barrier and a ventilated upwind barrier. To obtain data on the oscillatory force effect, traces were obtained with a strain amplifier and a Brush oscillograph.



Figure 24. Equipment Used For Obtaining Oscillograph Traces

This equipment is illustrated in figure 24. The oscillograph traces were obtained for treatment combinations 16, 20, 21, 26, 27, 30, 31, 34, and 35. These treatments consisted of a system without an upwind barrier, and systems with solid and ventilated upwind barriers at different barrier spacings. The wind velocity at which the oscillograph traces were obtained was 35.64 ft/sec.

If the steady state shear is designated by P_s , the ratio of the oscillatory shear P_o , to P_s can be written (14, p. 168)

$$P_o/P_s = X_o/X_s (1 - m\omega^2/k)$$

where, P_o = oscillatory shear, lb_f ,

P_s = static shear, lb_f ,

X_o = amplitude of oscillatory trace measured from the mean, in,

X_s = amplitude of static trace, in,

m = mass of vibrating roof component, slugs,

k = stiffness of the masts under cantilevered end load, lb_f/ft ,

ω = frequency of the applied oscillatory force, rad/sec.

X_o , X_s , and ω were found from the oscillograph traces. The stiffness $k = 747.34 lb_f/ft$ was found by plotting the load versus deflection curve for the masts. The mass $m = 2.211/32.2$ slugs, of the roof component was found by weighing the roof component. ω was found to be equal to 50π rad/sec for each of the treatments.

The oscillatory data are tabulated in table IX. A comparison of the ratios of P_o/P_s reveals that the smallest value of the ratio occurred with a system with no upwind barrier present. This means that the oscillatory force on a shelter without an upwind barrier was less than the oscillatory force on shelters with upwind barriers present. The ratios of P_o/P_s with ventilated upwind barriers present

TABLE IX
OSCILLATORY FORCE DATA

Treatment Number	Barrier Treatment	π_4	X_o in.	X_s in.	X_o/X_s	P_o/P_s
16	none	-	0.13	0.82	0.159	-0.201
20	solid	2	0.14	0.84	0.167	-0.211
21	open	2	0.14	0.82	0.171	-0.216
26	solid	8	0.26	0.92	0.283	-0.358
27	open	8	0.14	0.82	0.171	-0.216
30	solid	12	0.28	0.86	0.326	-0.412
31	open	12	0.15	0.80	0.188	-0.238
34	solid	16	0.28	0.88	0.318	-0.402
35	open	16	0.14	0.78	0.179	-0.226

were slightly greater than the ratio for a shelter without an upwind barrier. However, when solid upwind barriers were present, and with a barrier spacing to eaves height ratio of eight or greater, the values for the P_o/P_s ratio were much greater than the values of the ratio with a ventilated barrier or no barrier. For treatments 30 and 31, with $\pi_4 = 12$, the P_o/P_s value with a solid barrier was 1.74 times greater than the value of the ratio with a ventilated barrier under the same conditions. The frequency of the applied oscillatory force was greater than the natural frequency of the system, thereby resulting in negative values for the ratio P_o/P_s .

CHAPTER VIII

SUMMARY AND CONCLUSIONS

An experimental investigation of the gross horizontal and overturning wind forces on umbrella-type shelters was conducted, using models in a wind tunnel, exposed to a one-dimensional flow pattern blowing normal to the length of the models. The effects of variations in roof slope, shelter height, shelter length, and upwind barriers were investigated. The experimental investigation was organized and conducted according to the principles of similitude.

The following conclusions were drawn from the investigation:

1. When analyzing the horizontal and overturning wind forces on open or umbrella-type shelters, more emphasis should be placed on the shelter length and upwind barrier conditions than on roof slope and shelter height.

2. The wind force parameters on sharp-edged open or umbrella-type shelters are independent of Reynolds number. Therefore, the results obtained from a model study are valid for geometrically similar prototype structures.

3. A solid upwind barrier with a height equal to $1/2$ the eaves height reduced the wind forces on umbrella-type shelters an average of 27.9 per cent as compared to no upwind barrier. The reduction in forces on the shelter due to a solid upwind barrier was dependent upon the spacing between the shelter and the upwind barrier. The maximum force on a shelter without an upwind barrier was 2.8 times

greater than the forces on the same shelter with an upwind barrier. With two exceptions the minimum force on umbrella shelters occurred with a barrier spacing to eaves height ratio of two. For one shelter configuration, the force on the shelter with a solid upwind barrier was 1.024 times greater than the force on the same shelter configuration without an upwind barrier. This occurred with a barrier spacing to eaves height ratio of 14.

4. A ventilated upwind barrier with a uniformly distributed open area of approximately 50 per cent of the gross area and height of $1/2$ the eaves height reduced the wind forces on the umbrella shelters an average of only 5.4 per cent. The reduction in forces on the shelter due to the ventilated upwind barrier was independent of the spacing between the shelter and the barrier.

5. For open or umbrella-type shelters, the bending moment in the supporting masts was usually zero near the ground. Maximum moment usually occurred at the eaves level.

6. Wind pressure data obtained from experiments conducted on wind-tight structures are not applicable to open or umbrella-type shelters.

7. The wind force on umbrella-type shelters with $5/12$ and $7/12$ roof slopes was approximately the same when the shelter was exposed to either a one-dimensional or two-dimensional velocity profile. However, the wind force on an umbrella-type shelter with a $3/12$ roof slope was 19.5 per cent smaller for the two-dimensional velocity profile as compared to the one-dimensional velocity profile.

8. The oscillatory forces on umbrella-type shelters are relatively small in comparison to the steady state forces. However, the oscillatory forces are superimposed on the steady state forces, and hence

could become important. The oscillatory forces are greater when a solid upwind barrier is present as compared to no upwind barrier and a ventilated upwind barrier.

Suggestions For Future Investigations

1. The evaluation of the gross horizontal and overturning wind forces on open or umbrella-type shelters for different orientations of the shelter with respect to the wind direction.
2. The evaluation of the uplift forces on open or umbrella-type shelters due to wind.

SELECTED BIBLIOGRAPHY

1. Bridgman, P. W. Dimensional Analysis. Rev. ed. 2nd. pr. New Haven, Yale University Press. 1937.
2. Brooks, Fredrick A. An Introduction To Physical Microclimatology. Davis, California: University of California. 1959.
3. Buckingham, E. "On Physically Similar Systems, Illustrations of the Use of Dimensional Equations." The Physical Review. Series II, vol. IV, 4:345-376. 1914.
4. Collins, George F. "Determining Basic Windloads." Proceedings, American Society of Civil Engineers. 81:825.1-825.13. 1955.
5. Court, Arnold. "Wind Extremes as Design Factors." Journal of The Franklin Institute. 256:39-56. 1953.
6. Dodge, J. Robert, and Molander, E. Gordon. "Preventing Storm Wind Damage to Farm Buildings." United States Department of Agriculture. Agriculture Information Bulletin No. 144. July 1956.
7. Geiger, Rudolf. The Climate Near The Ground. Translated by Milroy Stewart and others. Cambridge, Mass., Harvard University Press. 1950.
8. "Influence of a Field Windbreak on Summer Wind Movement and Air Temperature." Manhattan, Agriculture Experiment Station, Kansas State University of Agriculture and Applied Science. Technical Bulletin 100. June 1959.
9. Irminger, J. O. V., and Nøkkentved, Chr. Wind-Pressure on Buildings. Experimental Researches, (first series). Translated by Alexander C. Jarvis and O. Brødsgaard. Danmarks Naturvidenskabelige Samfund, Ingeniørvidenskabelige Skrifter. A, Nr. 23. Copenhagen, Denmark. 1930.
10. _____ and _____ Wind-Pressure on Buildings. Experimental Researches, (second series). Translated by Alexander C. Jarvis and O. Brødsgaard, Danmarks Naturvidenskabelige Samfund. Ingeniørvidenskabelige Skrifter. A, Nr. 42. Copenhagen, Denmark. 1936.
11. Jensen, Martin. Shelter Effect. Copenhagen, Denmark, The Danish Technical Press. 1954.
12. Malina, Frank J. "Recent Developments in the Dynamics of Wind Erosion." Trans. American Geophysical Union. 22:262-284. 1941.

13. Murphy, Glenn. Similitude In Engineering. New York, The Roland Press Co. 1950.
14. Nelson, Gordon Leon. Wind Effects on Open-Front Livestock Shelters. Dissertation. Two copies of the complete thesis are on file at the Iowa State College Library. 1957.
15. Otis, C. K. "Causes of Barn Failures Due to Wind." Agricultural Engineering. 24:115-118. 1943.
16. Pagon, W. Walters, and Others. "Discussion of Variation of Wind Velocity and Gusts With Height." Proceedings, American Society of Civil Engineers. 79:Discussions. D-126:1-20. 1953.
17. Prandtl, Ludwig. Essentials of Fluid Dynamics. New York, Hafner Publishing Company. 1952.
18. Rogers, Paul, and Others. "Discussions of Wind-Load Standards in Europe." Proceedings, American Society of Civil Engineers. 77, No. D-42:1-9. 1951.
19. Sherlock, R. H. "Variation of Wind Velocity and Gusts With Height." Proceedings, American Society of Civil Engineers. 78:No. 126:1-26. 1952.
20. Snedecor, George W. Statistical Methods. 5th ed. The Iowa State College Press, Ames, Iowa. 1956.
21. Steel Construction. A manual for architects, engineers, and fabricators of buildings and other steel structures. American Institute of Steel Construction. New York, New York. 5th ed. 1956.
22. Sutton, O. G. Micrometeorology. New York. Mc Graw-Hill Book Company, Inc. 1953.
23. Theakston, F. H., and Walpole, E. W. "Wind Damage to Farm Buildings." Paper presented at the North Atlantic Section Meeting, ASAE. Storrs, Conn. Department of Agricultural Engineering, Ontario Agricultural College. Mimeo Rept. Guelph, Canada. (ca. 1955)
24. Thom, H. C. S. "Frequency of Maximum Wind Speeds." Proceedings, American Society of Civil Engineers. 80:part 5: No. 539:539.1-539.11. Nov., Dec. 1954.
25. Thornthwaite, C. W., and Halstead, Maurice. "Note on Variation of Wind With Height in the Layer Near the Ground." Trans., American Geophysical Union. 23:249-255. 1942.
26. Van Erp, John W. T. "Wind Load Standards in Europe." Proceedings, American Society of Civil Engineers. 76: No. 42:1-11. 1950.

27. Wilson, J. A. "Windstorms and Their Effect on Buildings." Journal of the Boston Society of Civil Engineers. 38:262-271. 1951.
28. "Wind and Snow Loads on Farm Structures." U. S. Department of Agriculture. Agricultural Research Service Leaflet ARS-42-5. 1956.
29. Zingg, Austin W. "A Study of the Movement of Surface Winds." Agricultural Engineering. 30:11-13. 1949.

APPENDIXES

APPENDIX A

EXPERIMENTAL DATA

Treat. No.	Vel. ft/sec	Avg. mom. at gages ft-lb			Avg. shear lbs	π_7	π_8	π_9
		top	mid.	bot.				
1	16.10	0.1709	0.1391	0.1189	0.0130	23,147	1.7458	0.6470
1	22.76	0.3243	0.2693	0.2474	0.0192	32,722	1.7458	0.6470
1	30.04	0.5894	0.4945	0.4378	0.0379	43,189	1.7458	0.6470
1	35.28	0.8160	0.6893	0.5910	0.0563	50,722	1.7458	0.6470
2	15.38	0.1651	0.1555	0.1448	0.0102	22,107	4.5644	0.5927
2	19.29	0.2610	0.2514	0.2359	0.0126	27,727	4.5644	0.5927
2	23.20	0.3607	0.3543	0.3333	0.0137	33,348	4.5644	0.5927
2	25.89	0.4582	0.4421	0.4158	0.0212	37,124	4.5644	0.5927
2	29.71	0.6066	0.5842	0.5380	0.0343	42,705	4.5644	0.5927
3	15.58	0.0800	0.0599	0.0507	0.0073	22,185	1.4847	0.2312
3	23.68	0.1567	0.1241	0.1067	0.0125	33,720	1.4847	0.2312
3	30.01	0.2512	0.2010	0.1712	0.0200	42,734	1.4847	0.2312
3	35.96	0.3542	0.2885	0.2630	0.0228	51,207	1.4847	0.2312
4	15.97	0.1608	0.1386	0.1200	0.0204	23,268	1.7750	0.4855
4	23.04	0.3692	0.3014	0.2650	0.0261	33,569	1.7750	0.4855
4	29.71	0.6144	0.5196	0.4551	0.0398	43,287	1.7750	0.4855
4	36.17	0.8817	0.7372	0.6620	0.0549	52,700	1.7750	0.4855
5	15.31	0.1123	0.0953	0.0818	0.0076	22,307	1.5089	0.6134
5	18.39	0.1613	0.1283	0.1078	0.0134	26,794	1.5089	0.6134
5	23.06	0.2518	0.2067	0.1764	0.0189	33,598	1.5089	0.6134
5	25.82	0.3164	0.2514	0.1938	0.0307	37,619	1.5089	0.6134
5	29.81	0.4116	0.3382	0.2822	0.0324	43,433	1.5089	0.6134
6	13.25	0.1165	0.0956	0.0825	0.0085	19,252	1.7611	0.6592
6	19.06	0.2389	0.2135	0.1823	0.0142	27,694	1.7611	0.6592
6	23.00	0.3667	0.3082	0.2558	0.0277	33,419	1.7611	0.6592
6	26.22	0.4298	0.3621	0.3157	0.0285	38,098	1.7611	0.6592
6	30.13	0.6348	0.5363	0.4714	0.0409	43,779	1.7611	0.6592
7	15.32	0.0606	0.0510	0.0445	0.0081	22,021	1.9722	0.3015
7	19.48	0.0815	0.0697	0.0644	0.0086	28,001	1.9722	0.3015
7	22.87	0.1088	0.0954	0.0858	0.0115	32,873	1.9722	0.3015
7	26.31	0.1425	0.1206	0.1093	0.0166	37,818	1.9722	0.3015

Treat. No.	Vel. ft/sec	Avg. mom. at gages ft-lb			Avg. shear lbs	π_7	π_8	π_9
		top	mid.	bot.				
8	15.32	0.1502	0.1411	0.1341	0.0081	22,021	4.2500	0.4648
8	18.88	0.2359	0.2230	0.2101	0.0129	27,138	4.2500	0.4648
8	23.03	0.3388	0.3211	0.3055	0.0167	33,103	4.2500	0.4648
8	26.39	0.4487	0.4224	0.4031	0.0228	37,933	4.2500	0.4648
9	15.09	0.0779	0.0655	0.0574	0.0103	21,482	1.9556	0.4756
9	19.89	0.1138	0.0993	0.0875	0.0132	28,315	1.9556	0.4756
9	23.21	0.1619	0.1395	0.1233	0.0193	33,041	1.9556	0.4756
9	26.78	0.2268	0.1952	0.1770	0.0249	38,124	1.9556	0.4756
10	15.63	0.1700	0.1598	0.1485	0.0108	22,188	3.4222	0.6034
10	19.93	0.2692	0.2483	0.2322	0.0185	28,293	3.4222	0.6034
10	22.96	0.3404	0.3217	0.2987	0.0209	32,594	3.4222	0.6034
10	26.62	0.4701	0.4488	0.4134	0.0284	37,790	3.4222	0.6034
11	29.54	0.0268	0.0134	0.0080	0.0094	28,051	0.7917	0.4605
11	36.39	0.0401	0.0214	0.0134	0.0134	34,556	0.7917	0.4605
11	41.29	0.0508	0.0295	0.0188	0.0160	39,209	0.7917	0.4605
11	46.72	0.0685	0.0407	0.0257	0.0214	44,365	0.7917	0.4605
12	29.87	0.0354	0.0204	0.0107	0.0124	28,364	0.8021	0.4924
12	36.06	0.0498	0.0279	0.0188	0.0155	34,243	0.8021	0.4924
12	40.86	0.0664	0.0364	0.0241	0.0212	38,801	0.8021	0.4924
12	46.98	0.0830	0.0504	0.0354	0.0238	44,612	0.8021	0.4924
13	29.71	0.0268	0.0188	0.0151	0.0059	28,171	1.0875	0.2455
13	35.96	0.0386	0.0295	0.0231	0.0078	34,097	1.0875	0.2455
13	40.65	0.0504	0.0392	0.0306	0.0099	38,544	1.0875	0.2455
13	47.70	0.0563	0.0440	0.0322	0.0121	45,229	1.0875	0.2455
14	29.81	0.0215	0.0134	0.0081	0.0067	28,156	0.9229	0.2308
14	36.14	0.0322	0.0204	0.0118	0.0102	34,134	0.9229	0.2308
14	40.78	0.0429	0.0311	0.0215	0.0107	38,157	0.9229	0.2308
14	47.16	0.0553	0.0450	0.0322	0.0116	44,542	0.9229	0.2308
15	28.73	0.0268	0.0182	0.0107	0.0081	27,135	0.9104	0.4125
15	35.33	0.0429	0.0293	0.0204	0.0113	33,369	0.9104	0.4125
15	41.10	0.0536	0.0381	0.0269	0.0134	38,819	0.9104	0.4125
15	46.97	0.0750	0.0542	0.0359	0.0196	44,363	0.9104	0.4125
16	21.94	0.1399	0.0921	0.0520	0.0220	31,162	0.8089	0.6377
16	28.88	0.2364	0.1538	0.0858	0.0377	41,018	0.8089	0.6377
16	35.37	0.3546	0.2334	0.1341	0.0552	50,236	0.8089	0.6377
16	40.92	0.4885	0.3158	0.1814	0.0768	58,119	0.8089	0.6377
17	23.04	0.1607	0.1409	0.1179	0.0214	33,523	1.7378	0.6022
17	29.24	0.2684	0.2421	0.2009	0.0338	42,544	1.7378	0.6022
17	35.62	0.4082	0.3599	0.2920	0.0546	51,827	1.7378	0.6022
17	40.70	0.5383	0.4821	0.3975	0.0704	59,219	1.7378	0.6022

Treat. No.	Vel. ft/sec	Avg. mom. at gages ft-lb			Avg. shear lbs	π_7	π_8	π_9
		top	mid.	bot.				
18	23.92	0.1342	0.0869	0.0606	0.0184	33,156	0.9278	0.4537
18	31.85	0.2184	0.1534	0.1006	0.0295	44,148	0.9278	0.4537
18	39.65	0.3103	0.2212	0.1508	0.0399	54,960	0.9278	0.4537
18	43.54	0.4413	0.3129	0.2307	0.0594	60,352	0.9278	0.4537
19	23.49	0.1547	0.1005	0.0607	0.0235	33,091	0.8389	0.6436
19	30.56	0.2695	0.1797	0.1093	0.0401	43,051	0.8389	0.6436
19	36.46	0.3831	0.2571	0.1515	0.0579	51,362	0.8389	0.6436
19	41.66	0.5059	0.3313	0.1997	0.0766	58,688	0.8389	0.6436
20	23.00	0.1363	0.1001	0.0631	0.0183	31,664	0.9944	0.4734
20	31.83	0.2578	0.1895	0.1298	0.0320	43,820	0.9944	0.4734
20	36.70	0.3473	0.2525	0.1740	0.0433	50,525	0.9944	0.4734
20	42.28	0.4483	0.3410	0.2288	0.0549	58,207	0.9944	0.4734
21	23.94	0.1642	0.1104	0.0706	0.0234	33,496	0.8667	0.6248
21	29.98	0.2511	0.1752	0.1061	0.0363	41,947	0.8667	0.6248
21	36.91	0.3872	0.2584	0.1613	0.0565	51,644	0.8667	0.6248
21	42.52	0.5403	0.3701	0.2249	0.0789	59,493	0.8667	0.6248
22	24.20	0.1781	0.1312	0.0895	0.0222	33,269	0.9722	0.5854
22	31.04	0.3041	0.2178	0.1534	0.0377	42,672	0.9722	0.5854
22	37.43	0.4381	0.3213	0.2260	0.0530	51,457	0.9722	0.5854
22	42.83	0.5828	0.4142	0.2841	0.0747	58,880	0.9722	0.5854
23	23.42	0.1647	0.1018	0.0730	0.0229	32,769	0.8778	0.6214
23	30.57	0.2830	0.1819	0.1139	0.0423	42,773	0.8778	0.6214
23	36.67	0.3898	0.2731	0.1753	0.0559	51,308	0.8778	0.6214
23	42.62	0.5569	0.3825	0.2398	0.0793	59,634	0.8778	0.6214
24	24.85	0.1884	0.1341	0.0906	0.0245	34,720	0.9722	0.5725
24	31.39	0.3098	0.2244	0.1504	0.0399	43,858	0.9722	0.5725
24	37.60	0.4455	0.3140	0.2186	0.0567	52,534	0.9722	0.5725
24	41.98	0.5517	0.4029	0.2728	0.0697	58,655	0.9722	0.5725
25	23.82	0.1628	0.1142	0.0708	0.0230	33,405	0.8944	0.6021
25	29.58	0.2614	0.1798	0.1168	0.0362	41,483	0.8944	0.6021
25	35.32	0.3775	0.2672	0.1649	0.0532	49,532	0.8944	0.6021
25	42.11	0.5426	0.3721	0.2388	0.0760	59,055	0.8944	0.6021
26	24.27	0.1734	0.1162	0.0787	0.0237	33,910	0.9311	0.5833
26	31.61	0.3008	0.1983	0.1380	0.0407	44,165	0.9311	0.5833
26	37.34	0.4347	0.3056	0.2151	0.0549	52,171	0.9311	0.5833
26	43.34	0.5691	0.4099	0.2673	0.0755	60,555	0.9311	0.5833
27	23.09	0.1420	0.1040	0.0651	0.0192	32,428	0.9067	0.5709
27	29.77	0.2581	0.1796	0.1134	0.0362	41,809	0.9067	0.5709
27	36.46	0.4048	0.2719	0.1752	0.0574	51,204	0.9067	0.5709
27	41.81	0.5334	0.3690	0.2431	0.0726	58,718	0.9067	0.5709

Treat. No.	Vel. ft/sec	Avg. mom. at gages ft-lb			Avg. shear lbs	π_7	π_8	π_9
		top	mid.	bot.				
28	24.37	0.1564	0.1064	0.0716	0.0212	34,001	0.9344	0.6192
28	30.41	0.2506	0.1805	0.1196	0.0328	42,428	0.9344	0.6192
28	37.08	0.4046	0.2792	0.1851	0.0549	51,734	0.9344	0.6192
28	42.91	0.5555	0.4034	0.2599	0.0739	59,868	0.9344	0.6192
29	23.17	0.1442	0.0971	0.0580	0.0216	32,410	0.8722	0.6117
29	30.11	0.2506	0.1758	0.1061	0.0361	42,118	0.8722	0.6117
29	36.28	0.3781	0.2576	0.1557	0.0556	50,748	0.8722	0.6117
29	42.11	0.5026	0.3402	0.2166	0.0715	58,903	0.8722	0.6117
30	23.98	0.1446	0.1020	0.0607	0.0210	33,781	0.9089	0.5678
30	30.36	0.2527	0.1696	0.1102	0.0356	42,768	0.9089	0.5678
30	37.17	0.3979	0.2795	0.1825	0.0539	52,361	0.9089	0.5678
30	42.78	0.5132	0.3732	0.2381	0.0688	60,264	0.9089	0.5678
31	23.29	0.1459	0.0956	0.0586	0.0218	32,226	0.8667	0.6013
31	29.98	0.2464	0.1648	0.1007	0.0364	41,483	0.8667	0.6013
31	36.08	0.3616	0.2566	0.1605	0.0503	49,923	0.8667	0.6013
31	42.12	0.5091	0.3540	0.2144	0.0737	58,281	0.8667	0.6013
32	23.57	0.1430	0.0968	0.0639	0.0198	32,979	0.8667	0.6534
32	30.86	0.2719	0.1786	0.1042	0.0419	43,179	0.8667	0.6534
32	36.55	0.3848	0.2601	0.1633	0.0554	51,140	0.8667	0.6534
32	42.67	0.5499	0.3683	0.2375	0.0781	59,703	0.8667	0.6534
33	23.82	0.1388	0.0988	0.0554	0.0209	33,233	0.8511	0.6118
33	29.91	0.2473	0.1597	0.1066	0.0367	41,730	0.8511	0.6118
33	36.48	0.3905	0.2496	0.1531	0.0594	50,897	0.8511	0.6118
33	41.77	0.5044	0.3447	0.2138	0.0727	58,278	0.8511	0.6118
34	24.20	0.1438	0.1049	0.0620	0.0205	34,090	0.9056	0.5895
34	30.04	0.2384	0.1617	0.1071	0.0328	42,317	0.9056	0.5895
34	36.96	0.3671	0.2573	0.1634	0.0509	52,066	0.9056	0.5895
34	41.20	0.4710	0.3283	0.2055	0.0664	58,038	0.9056	0.5895
35	23.56	0.1359	0.0981	0.0550	0.0202	32,871	0.8500	0.6794
35	30.86	0.2560	0.1617	0.1046	0.0379	43,056	0.8500	0.6794
35	36.40	0.3797	0.2600	0.1480	0.0579	50,785	0.8500	0.6794
35	42.16	0.5204	0.3703	0.2167	0.0759	58,822	0.8500	0.6794
36	15.24	0.0669	0.0600	0.0525	0.0072	22,174	2.5194	0.4101
36	23.31	0.1650	0.1495	0.1366	0.0142	33,916	2.5194	0.4101
36	29.82	0.2812	0.2507	0.2303	0.0255	43,388	2.5194	0.4101
36	35.95	0.4151	0.3776	0.3385	0.0383	52,307	2.5194	0.4101
37	15.42	0.0787	0.0643	0.0536	0.0126	22,436	1.6588	0.5455
37	23.04	0.1713	0.1489	0.1232	0.0241	33,523	1.6588	0.5455
37	29.96	0.2892	0.2518	0.2100	0.0396	43,592	1.6588	0.5455
37	35.49	0.4043	0.3637	0.3043	0.0500	51,638	1.6588	0.5455

Treat. No.	Vel. ft/sec	Avg. mom. at gages ft-lb			Avg. shear lbs	π_7	π_8	π_9
		top	mid.	bot.				
38	15.21	0.0643	0.0536	0.0429	0.0107	21,919	1.7639	0.5692
38	23.13	0.1564	0.1356	0.1163	0.0201	33,332	1.7639	0.5692
38	29.79	0.2636	0.2325	0.2063	0.0287	42,930	1.7639	0.5692
38	34.67	0.3654	0.3225	0.2679	0.0488	49,963	1.7639	0.5692
39	15.21	0.0702	0.0616	0.0509	0.0097	21,919	1.8056	0.5890
39	22.74	0.1671	0.1484	0.1248	0.0212	32,771	1.8056	0.5890
39	29.72	0.2935	0.2625	0.2185	0.0375	42,829	1.8056	0.5890
39	34.38	0.3947	0.3542	0.2984	0.0482	49,545	1.8056	0.5890
40	23.04	0.0365	0.0279	0.0188	0.0089	21,658	0.9333	0.5071
40	29.79	0.0643	0.0450	0.0296	0.0174	28,002	0.9333	0.5071
40	35.78	0.0884	0.0643	0.0387	0.0249	33,633	0.9333	0.5071
40	40.03	0.1099	0.0847	0.0553	0.0273	37,628	0.9333	0.5071
41	23.69	0.0407	0.0285	0.0204	0.0102	22,425	1.0208	0.3677
41	30.34	0.0670	0.0483	0.0376	0.0147	28,720	1.0208	0.3677
41	36.39	0.0922	0.0697	0.0510	0.0206	34,447	1.0208	0.3677
41	41.66	0.1223	0.0912	0.0697	0.0263	39,435	1.0208	0.3677
42	22.38	0.0343	0.0285	0.0215	0.0064	21,185	1.1188	0.4712
42	29.78	0.0644	0.0520	0.0344	0.0150	28,189	1.1188	0.4712
42	35.68	0.0928	0.0788	0.0569	0.0180	33,775	1.1188	0.4712
42	41.70	0.1292	0.1019	0.0741	0.0276	39,473	1.1188	0.4712
43	22.66	0.0418	0.0311	0.0215	0.0102	21,450	1.0021	0.5428
43	30.03	0.0745	0.0531	0.0392	0.0177	28,426	1.0021	0.5428
43	35.99	0.1110	0.0794	0.0590	0.0260	34,068	1.0021	0.5428
43	40.51	0.1362	0.1057	0.0762	0.0300	38,346	1.0021	0.5428
44	23.04	0.0418	0.0322	0.0215	0.0102	21,809	1.0333	0.4618
44	29.63	0.0670	0.0547	0.0370	0.0150	28,047	1.0333	0.4618
44	36.14	0.1029	0.0852	0.0580	0.0225	34,210	1.0333	0.4618
44	41.43	0.1340	0.1105	0.0735	0.0303	39,217	1.0333	0.4618
45	22.95	0.0568	0.0429	0.0322	0.0123	22,179	0.9896	0.5807
45	29.43	0.0965	0.0750	0.0499	0.0233	28,441	0.9896	0.5807
45	35.50	0.1436	0.1083	0.0724	0.0356	34,307	0.9896	0.5807
45	41.02	0.1972	0.1495	0.0971	0.0501	39,641	0.9896	0.5807
46	23.21	0.0546	0.0429	0.0322	0.0112	22,430	1.0958	0.4287
46	29.96	0.0966	0.0750	0.0536	0.0215	28,953	1.0958	0.4287
46	35.78	0.1355	0.1083	0.0804	0.0276	34,578	1.0958	0.4287
46	41.33	0.1822	0.1452	0.1072	0.0375	39,941	1.0958	0.4287
47	23.00	0.0632	0.0499	0.0322	0.0155	22,227	1.0271	0.4595
47	29.50	0.1018	0.0831	0.0547	0.0236	28,509	1.0271	0.4595
47	35.86	0.1501	0.1260	0.0848	0.0327	34,655	1.0271	0.4595
47	41.11	0.2047	0.1645	0.1110	0.0469	39,729	1.0271	0.4595

Treat. No.	Vel. ft/sec	Avg. mom. at gages ft-lb			Avg. shear lbs	π_7	π_8	π_9
		top	mid.	bot.				
48	22.87	0.0675	0.0509	0.0343	0.0166	22,101	0.9937	0.5539
48	29.47	0.1179	0.0900	0.0590	0.0295	28,480	0.9937	0.5539
48	35.16	0.1629	0.1276	0.0911	0.0359	33,978	0.9937	0.5539
48	41.54	0.2331	0.1715	0.1222	0.0555	40,142	0.9937	0.5539
49	22.89	0.0616	0.0466	0.0322	0.0147	22,121	1.0063	0.5438
49	29.63	0.1087	0.0841	0.0573	0.0257	28,634	1.0063	0.5438
49	36.00	0.1623	0.1297	0.0868	0.0378	34,790	1.0063	0.5438
49	41.50	0.2207	0.1730	0.1190	0.0509	40,105	1.0063	0.5438
50	23.41	0.0520	0.0144	-0.0307	0.0207	32,615	0.4022	0.6075
50	29.82	0.0885	0.0191	-0.0491	0.0344	41,545	0.4022	0.6075
50	35.96	0.1334	0.0328	-0.0694	0.0507	50,099	0.4022	0.6075
50	41.41	0.1823	0.0440	-0.0928	0.0688	57,692	0.4022	0.6075
51	23.29	0.0803	0.0605	0.0322	0.0241	33,062	0.8722	0.5545
51	29.88	0.1307	0.1055	0.0589	0.0359	42,417	0.8722	0.5545
51	35.73	0.1837	0.1430	0.0847	0.0495	50,722	0.8722	0.5545
51	41.48	0.2517	0.1966	0.1109	0.0704	58,885	0.8722	0.5545
52	24.58	0.0645	0.0253	-0.0147	0.0198	34,109	0.4800	0.5109
52	30.80	0.1089	0.0418	-0.0220	0.0327	42,740	0.4800	0.5109
52	37.07	0.1567	0.0590	-0.0303	0.0468	51,441	0.4800	0.5109
52	40.66	0.1888	0.0714	-0.0346	0.0559	56,423	0.4800	0.5109
53	23.57	0.0562	0.0146	-0.0213	0.0194	32,614	0.4267	0.6145
53	29.86	0.0939	0.0233	-0.0393	0.0333	41,317	0.4267	0.6145
53	36.48	0.1475	0.0345	-0.0600	0.0519	50,477	0.4267	0.6145
53	42.25	0.2021	0.0522	-0.0807	0.0707	58,461	0.4267	0.6145
54	24.91	0.0654	0.0228	-0.0125	0.0195	34,804	0.4833	0.5165
54	30.14	0.1004	0.0389	-0.0193	0.0299	42,111	0.4833	0.5165
54	36.70	0.1506	0.0563	-0.0303	0.0452	51,277	0.4833	0.5165
54	42.84	0.2112	0.0819	-0.0376	0.0622	59,856	0.4833	0.5165
55	23.81	0.0629	0.0158	-0.0207	0.0209	33,267	0.4389	0.5837
55	30.26	0.1019	0.0281	-0.0335	0.0339	42,279	0.4389	0.5837
55	36.73	0.1559	0.0455	-0.0513	0.0518	51,319	0.4389	0.5837
55	42.34	0.2092	0.0663	-0.0690	0.0696	59,157	0.4389	0.5837
56	23.38	0.0755	0.0536	0.0429	0.0163	33,059	1.0667	0.4965
56	29.47	0.1275	0.0965	0.0723	0.0276	41,670	1.0667	0.4965
56	36.14	0.1858	0.1404	0.1045	0.0407	51,101	1.0667	0.4965
56	40.46	0.2474	0.1881	0.1377	0.0549	57,210	1.0667	0.4965
57	23.36	0.0803	0.0616	0.0349	0.0227	33,031	0.8806	0.6012
57	29.61	0.1269	0.0975	0.0584	0.0343	41,868	0.8806	0.6012
57	36.14	0.1976	0.1484	0.0911	0.0533	51,101	0.8806	0.6012
57	40.40	0.2453	0.1859	0.1098	0.0678	57,125	0.8806	0.6012

Treat. No.	Vel. ft/sec	Avg. mom. at gages ft-lb			Avg. shear lbs	π_7	π_8	π_9
		top	mid.	bot.				
58	23.00	0.0750	0.0558	0.0348	0.0201	32,430	0.9694	0.4760
58	29.97	0.1297	0.1008	0.0643	0.0327	42,257	0.9694	0.4760
58	35.01	0.1864	0.1436	0.0991	0.0437	49,364	0.9694	0.4760
58	41.87	0.2635	0.2100	0.1425	0.0605	59,036	0.9694	0.4760
59	23.04	0.0819	0.0648	0.0429	0.0195	32,486	0.9472	0.5778
59	29.57	0.1382	0.1045	0.0669	0.0357	41,693	0.9472	0.5778
59	35.99	0.2073	0.1617	0.1028	0.0523	50,745	0.9472	0.5778
59	41.60	0.2731	0.2143	0.1404	0.0664	58,656	0.9472	0.5778

APPENDIX B

ANALYSIS OF VARIANCE TABLES

AOV due to differences in π_B for analysis 1. (Refer to table III for parameter combinations)

Source	Degrees freedom	Sum of squares	Mean square	Variance ratio	Sign. level
total	47	0.368136			
replication	2	0.000205			
π_3	3	0.142377	0.047459	18.7536	99.95
π_4	1	0.018240	0.018240	7.2076	99.90
π_6	1	0.002856	0.002856	1.1286	70.23
$\pi_3 \times \pi_4$	3	0.006044	0.002015	0.7962	-
$\pi_3 \times \pi_6$	3	0.104278	0.034759	13.7351	99.95
$\pi_4 \times \pi_6$	1	0.010624	0.010624	4.1981	95.00
remainder	33	0.083512	0.002531		

AOV due to differences in π_B for analysis 2. (Refer to table III for parameter combinations)

Source	Degrees freedom	Sum of squares	Mean square	Variance ratio	Sign. level
total	17	33.949700			
replication	2	0.0017658			
π_1	2	20.563100	10.2816	13,181.5	99.95
π_2	1	8.693300	8.6933	11,145.2	99.95
$\pi_1 \times \pi_2$	2	4.683700	2.3419	3,002.4	99.95
remainder	10	0.007800			

AOV due to differences in π_B for analysis 3. (Refer to table III for parameter combinations)

Source	Degrees freedom	Sum of squares	Mean square	Variance ratio	Sign. level
total	23	19.8515			
π_1	2	9.6831	4.8415	29.2538	99.95
π_2	1	5.1572	5.1572	31.1613	99.95
π_4	1	0.0879	0.0879	0.5311	-
π_6	1	0.3642	0.3642	2.2006	79.20
$\pi_1 \times \pi_2$	2	0.5940	0.2970	1.7946	75.40
$\pi_1 \times \pi_4$	2	0.0446	0.0223	0.0135	-
$\pi_1 \times \pi_6$	2	2.0759	1.0380	6.2719	97.74
$\pi_2 \times \pi_4$	1	0.0957	0.0957	0.5782	-
$\pi_2 \times \pi_6$	1	0.2559	0.2559	1.5462	73.10
$\pi_4 \times \pi_6$	1	0.0032	0.0032	0.0019	-
remainder	9	1.4898	0.1655		

AOV due to differences in π_B for analysis 4. (Refer to table III for parameter combinations)

Source	Degrees freedom	Sum of squares	Mean square	Variance ratio	Sign. level
total	29	30.80328			
treatment (barrier)	2	0.59190	0.29595	3.6426	95.00
π_1	2	15.45325	7.72663	95.0993	99.95
π_2	1	7.84672	7.84672	96.5774	99.95
treat. \times π_1	4	3.62720	0.90680	11.1609	99.95
treat. \times π_2	2	0.53084	0.26542	3.2668	93.12
$\pi_1 \times \pi_2$	2	1.45341	0.72671	8.9443	99.66
remainder	16	1.29996	0.08125		

AOV due to differences in π_q for analysis 1. (Refer to table III for parameter combinations)

Source	Degrees freedom	Sum of squares	Mean square	Variance ratio	Sign. level
total	47	118.088			
replication	2	0.831			
π_3	3	54.934	18.3245	12.4032	99.95
π_4	1	1.253	1.253	0.8480	-
π_6	1	1.083	1.083	0.7327	-
$\pi_3 \times \pi_4$	3	4.650	1.550	1.0492	60.44
$\pi_3 \times \pi_6$	3	1.521	0.507	0.3432	-
$\pi_4 \times \pi_6$	1	4.023	4.023	2.7231	88.30
remainder	33	48.754			

AOV due to differences in π_q for analysis 2. (Refer to table III for parameter combinations)

Source	Degrees freedom	Sum of squares	Mean square	Variance ratio	Sign. level
total	17	1.25734			
replication	2	0.11646			
π_1	2	0.29328	0.14664	3.5961	92.88
π_2	1	0.41474	0.41474	10.1710	99.03
$\pi_1 \times \pi_2$	2	0.02508	0.01254	0.3075	-
remainder	10	0.40778			

AOV due to differences in π_q for analysis 3. (Refer to table III for parameter combinations)

Source	Degrees freedom	Sum of squares	Mean square	Variance ratio	Sign. level
total	23	35.2304			
π_1	2	5.2452	2.6226	5.3305	96.85
π_2	1	0.0554	0.0554	1.1260	67.78
π_4	1	5.7053	5.7053	11.5961	99.17
π_6	1	7.0975	7.0975	14.4258	99.54
$\pi_1 \times \pi_2$	2	0.2120	0.1060	0.2154	-
$\pi_1 \times \pi_4$	2	7.1881	3.5940	7.3049	98.53
$\pi_1 \times \pi_6$	2	2.4695	1.2347	2.5096	83.86
$\pi_2 \times \pi_4$	1	0.2044	0.2044	0.4154	-
$\pi_2 \times \pi_6$	1	0.0474	0.0474	0.0963	-
$\pi_4 \times \pi_6$	1	2.5779	2.5779	5.2396	95.14
remainder	9	4.4277	0.4920		

AOV due to differences in π_q for analysis 4. (Refer to table III for parameter combinations)

Source	Degrees freedom	Sum of squares	Mean square	Variance ratio	Sign. level
total	29	18.15721			
treatment (barrier)	2	9.67374	4.83687	231.142	99.95
π_1	2	3.93168	1.96584	93.9424	99.95
π_2	1	0.13040	0.13040	6.2314	97.07
treat. $\times \pi_1$	4	3.85332	0.96330	46.0336	99.95
treat. $\times \pi_2$	2	0.08588	0.04299	2.0544	80.95
$\pi_1 \times \pi_2$	2	0.14738	0.07369	3.5215	94.43
remainder	16	0.33481	0.020926		

VITA

Charles E. Rice

Candidate For The Degree Of

Master of Science

Thesis: WIND FORCES ON OPEN OR UMBRELLA-TYPE SHELTERS

Major Field: Agricultural Engineering

Biographical:

Personal Data: Born near Seminole, Oklahoma, February 13, 1932,
the son of C. C. and Lilly A. Rice.

Education: Graduated from Pleasant Grove High, Seminole,
Oklahoma, in 1949. Attended Seminole Junior College in
1949-1950; received the Bachelor of Science degree in
Agricultural Engineering in May, 1960, from Oklahoma
State University. Completed the requirements for the
Master of Science Degree in May 1961.

Experience: Served as a graduate research assistant for the
Agricultural Engineering Department, Oklahoma State
University, for one one semester and a summer term.

Member of the American Society of Agricultural Engineers.